INTERIM REPORT

Accession No.______________

Contract Program or Project Title: SSC Code Development & Validation

Subject of this Document: An Air Blast Heat Exchanger System Model

Type of Document: Informal Report

Author(s): K. B. Cady

Date of Document: June, 1979

Responsible NRC Individual and NRC Office or Division: Dr. Robert T. Curtis, Chief
Analytical Advanced Reactor Safety Research Branch
Division of Reactor Safety Research
U.S. Nuclear Regulatory Commission
Washington, D.C. 20555

Brookhaven National Laboratory
Upton, NY 11973
Associated Universities, Inc.
for the
U.S. Department of Energy

Prepared for
U.S. Nuclear Regulatory Commission
Washington, D. C. 20555
Under Interagency Agreement EY-76-C-02-0016
NRC FIN No. A-3015-8

BNL-NUREG - 26237
INFORMAL REPORT

AN AIR BLAST HEAT EXCHANGER SYSTEM MODEL

K.B. CADY

NRC Research and Technical
Assistance Report

DATE PUBLISHED - JUNE 1979

DEPARTMENT OF NUCLEAR ENERGY BROOKHAVEN NATIONAL LABORATORY
UPTON, NEW YORK 11973

Prepared for the U.S. Nuclear Regulatory Commission
Office of Nuclear Regulatory Research
Contract No. EY-76-C-02-0016

516 061

516 062

BNL-NUREG 26237
Informal Report
Limited Distribution

AN AIR BLAST HEAT EXCHANGER SYSTEM MODEL

K.B. CADY*

DRAFT REPORT COMPLETED - DECEMBER 1978

DATE PUBLISHED - JUNE 1979

ENGINEERING AND ADVANCED REACTOR SAFETY DIVISION
DEPARTMENT OF NUCLEAR ENERGY
BROOKHAVEN NATIONAL LABORATORY
UPTON, NEW YORK 11973

*Work performed while author was on sabbatical leave from Cornell University, Ithaca, New York.

FOREWORD

An air blast heat exchanger code was developed at Brookhaven National Laboratory as part of the Super System Code (SSC) development project for simulating transients in liquid-metal-cooled fast breeder reactors (LMFBR's). It is intended to form a part of the SSC-L (loop) code and enable the SSC-L code to model the Fast Flux Test Facility (FFTF) where the tertiary heat removal system is an air dump heat exchanger.

This work, covered under budget activity No. 60-19-20-01, was performed for the Office of the Assistant Director for Advanced Reactor Safety Research, Division of Reactor Safety Research, United States Nuclear Regulatory Commission.

TABLE OF CONTENTS

516 065

LIST OF FIGURES

LIST OF TABLES

ACKNOWLEDGEMENT

The author wishes to thank the Engineering and Advanced Reactor Safety Division at Brookhaven National Laboratory for their support of this work performed while the author was on a six month sabbatical leave from Cornell University. In particular, he wishes to acknowledge the help of A. K. Agrawal, who defined and suggested the topic; M. Khatib-Rahbar, who gave valuable technical advice; K. R. Perkins, who helped with the understanding of the FFTF/DHX prototype experimental tests; J. Zahra, who supervises the computer terminal; E. S. Srinivasan, who converted the code to a form compatible with the Brookhaven SSC system code; and to W. Y. Kato and R. J. Cerbone, who arranged the author's stay at Brookhaven. The author also wishes to thank D. Clay for typing the manuscript.

The work was performed as part of the SSC code development work at Brookhaven National Laboratory under the auspices of the Unites States Nuclear Regulatory Commission.

1. ABSTRACT

An air blast sodium-to-air heat exchanger model is developed to provide a computer simulation of air dump heat exchangers similar to the Fast Flux Test Facility dump heat exchanger (DHX). The physical model includes the sodium-air heat transfer, buoyancy of the stack air causing natural convection, forced draft fans, finned tube air resistance, variable angle inlet fan vanes, fan motor, variable speed magnetic drive, fine and course outlet dampers and controllers which adjust the fan speed and damper positions. The model is developed and tested by choosing parameters for the FFTF DHX's and comparing heat exchange, flow rates, fan speeds, and air and sodium temperatures with experimental data from the FFTF/DHX prototype tests. These comparisons include 18 forced convection and five natural convection steady state tests and a fan coastdown test. All comparisons are excellent due in part to selecting some model parameters, such as heat transfer coefficients and friction coefficients, consistent with the test results.

A set of steady state forced and natural convection results are predicted for the FFTF DHX's and several sodium flow coastdown transients are analyzed. These transients demonstrate the response of the DHX and its control systems to sodium side flow changes. The model has been coded to be compatible with and form a part of the Brookhaven SSC-L code[†] for loop type liquid metal cooled fast reactor system simulations.

[†] A. K. Agrawal, et al., "An Advanced Thermohydraulic Simulation Code for Transients in LMFBRs (SSC-L Code)," Brookhaven National Laboratory, BNL-NUREG-50773 (1978).

516 065

2. INTRODUCTION

An air blast sodium heat exchanger model is developed to provide a computer simulation of air dump heat exchangers similar to the Fast Flux Test Facility dump heat exchanger (FFTF/DHX).[1,2,6] The transient model has the following major subroutines shown below and in Figure 1:

1) REST3T, a dummy subroutine which generates input process variables from the rest of plant (e.g., sodium flow rate, sodium inlet temperature).
2) HX3T, a subroutine which models the sodium-air heat transfer.
3) BUOY3T, a subroutine which models the buoyant stack draft.
4) CNTR3T, a subroutine which models the module controller (controlling damper positions) and the unit controller (controlling fan speed).
5) DRIV3T, a subroutine which models the fan motor and the variable speed magnetic drive.
6) FAN3T, a subroutine which models the fan, the finned tube air resistance, and the variable inlet vanes.
7) DAMP3T, a subroutine which models the fine and coarse outlet dampers.

These seven subroutines calculate the thirty-one process variables, appearing in Figure 1. The steady state version of the code has seven similar subroutines (e.g., REST3S, HX3S, BUOY3S) used for finding compatible, steady state values of the thirty-one process variables.

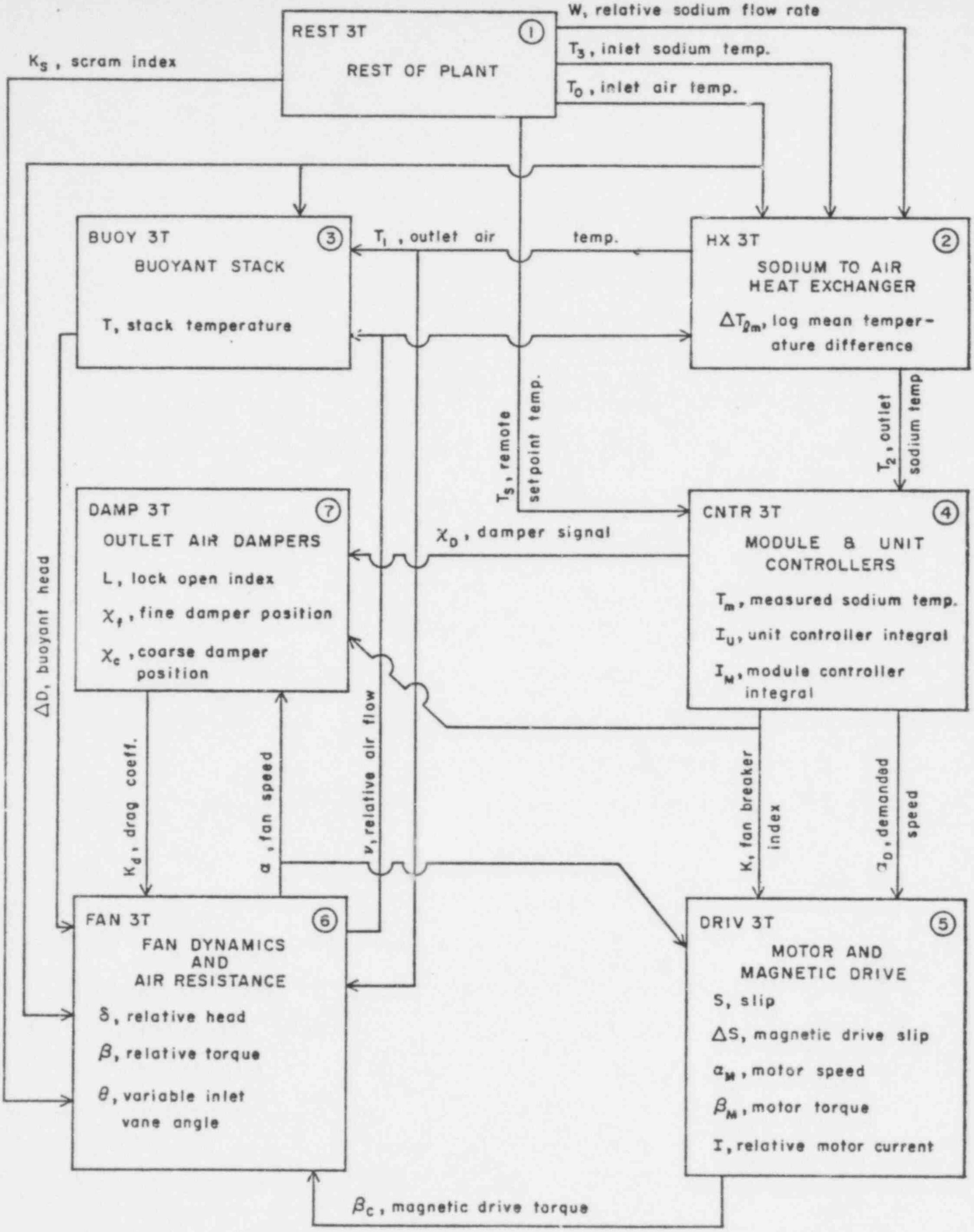

Figure 1. System Model Showing Major Subroutines and Process Variables.

516 071

3. HEAT EXCHANGE MODEL

The heat exchanger is modeled as a one-region, counter-flow, sodium-air heat exchanger. The following physical assumptions are made:

1) the residence time of the air flowing across the heated tube bundle is zero;

2) air is taken to be a perfect gas for the computation of specific heat and density:

$$C_p = \text{constant} \; , \tag{1}$$

$$\rho \propto \frac{1}{T} \; ; \tag{2}$$

3) Chapman-Enskogg theory using a Lennard-Jones potential gives the viscosity and thermal conductivity of air as a function of absolute temperature,[3]

$$\mu \propto k \propto T^{0.715} \; ; \tag{3}$$

4) heat transfer resistance on the air side dominates the overall heat transfer coefficient which is given by a modified Colburn equation,[4]

$$h \propto k \, Re^{0.70} \, Pr^{1/3} \; ; \text{ and} \tag{4}$$

5) the properties of air and sodium are taken at the average of the inlet and outlet air and sodium temperatures, respectively.

The subroutine HX3T is based on the energy conservation equations coupled with assumption 1) for air and sodium;

$$0 = (C_p\dot{m})_{air} \, (T_o - T_1) + UA \, \Delta T_{\ell m} \quad , \tag{5}$$

516 072

$$(C_p m)_{Na} \frac{dT_2}{dt} = (C_p \dot{m})_{Na} (T_3 - T_2) - UA \, \Delta T_{\ell m} \quad , \text{ and} \qquad (6)$$

$$\Delta T_{\ell m} \equiv \frac{(T_3 - T_1) - (T_2 - T_o)}{\ell n \frac{T_3 - T_1}{T_2 - T_o}} \quad , \qquad (7)$$

where the four temperatures are defined by Figure 2.

The steady-state model HX3S uses the same equations with the temperature derivative in Equation (6) set equal to zero. Using physical assumptions given above, heat transfer ratios are defined and given as

$$\xi_1 \equiv \frac{UA}{(C_p \dot{m})_{air}} = \frac{T_1 - T_o}{\Delta T_{\ell m}} = \xi_{1r} \, T^{0.21} \, \overline{\nu}^{0.30} \quad , \text{ and} \qquad (8)$$

$$\xi_2 \equiv \frac{UA}{(C_p \dot{m})_{Na}} = \frac{T_3 - T_2}{\Delta T_{\ell m}} = \xi_{1r} \frac{1}{rw} T^{0.21} \, \nu^{0.70} \quad , \qquad (9)$$

where

T is the mean absolute air temperature,

r is the sodium heat capacity,

ν is the air mass flow rate, and

w is the sodium mass flow rate,

all relative to their values at a reference state.

Table 1 shows eighteen steady state tests on the prototype DHX module for the "as built" FFTF HTS/DHX performed on June 16-21, 1975.[7] Test B15 is close to the design conditions and is taken as the reference state resulting in

$$\text{air} \begin{Bmatrix} C_p = 0.2402 \text{ Btu/lbm - }^{o}\text{F} \\ \dot{m} = 0.1995 \times 10^{7} \text{ lbm/hr} \\ \xi = 0.3895 \end{Bmatrix}$$

516 073

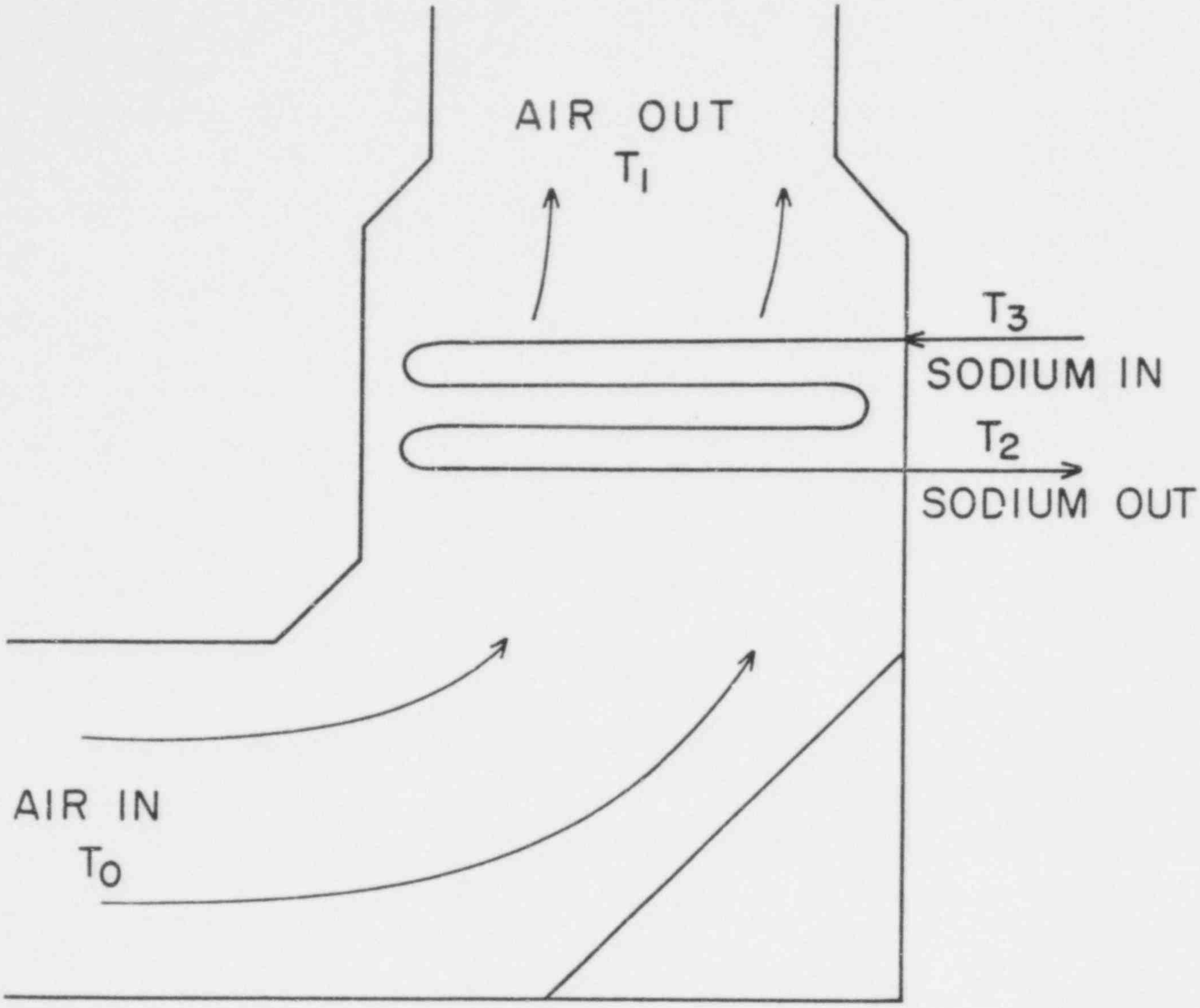

Figure 2. Air and Sodium Temperatures

516 074

TABLE 1

<u>As Built FFTF HTS/DHX Steady-State Test Data</u>

<u>June 16-21, 1975</u>[7]

(Predicted results in parentheses)

	SODIUM			AIR			HEAT TRANSFER	
Page (Ref.7)	Flow 10^7 lbm/hr	T_3 °F	T_2 °F	Flow[a] 10^7 lbm/hr	T_0 °F	T_1 °F	$\Delta T_{\ell m}$ °F	Power MWt
B4	.1168	688.3	(519.8) 519.5	.1277	58.4	(256.6) 257.7	(446.4) 445.6	(17.89) 17.92
B5	.1169	688.7	(519.4) 519.4	.1277	54.8	(254.1) 255.2	(449.4) 448.8	(17.99) 18.00
B6	.1169	688.9	(519.4) 519.2	.1277	54.0	(253.6) 254.7	(450.2) 449.5	(18.02) 18.04
B7	.1173	703.8	(519.7) 519.3	.1405	54.2	(251.8) 253.1	(458.7) 457.9	(19.62) 19.66
B8	.1170	724.1	(520.2) 519.1	.1598	65.0	(256.7) 258.5	(461.3) 459.8	(21.65) 21.76
B9	.1168	735.4	(520.2) 519.1	.1688	65.0	(256.0) 257.8	(467.2) 465.7	(22.78) 27.91
B10	.1168	744.8	(520.3) 519.3	.1762	64.1	(254.8) 256.6	(472.9) 471.5	(23.75) 23.87
B11	.1167	760.1	(520.8) 520.0	.1877	63.5	(254.0) 255.5	(481.3) 480.1	(25.27) 25.36
B13	.1162	772.0	(518.8) 519.2	.1960	55.7	(247.8) 248.5	(493.0) 497.9	(26.61) 26.59
B14	.1175	765.7	(516.3) 518.3	.2041	73.0	(256.8) 256.2	(475.4) 476.6	(26.52) 26.32
<u>B15</u>	.1163	771.3	(521.7) 521.7	.1995	72.7	(259.7) 259.7	(479.6) 47[illegible].6	(26.37) 26.27
B16	.0758	816.9	(560.2) 562.4	.1041	70.3	(308.4) 306.9	(49[illegible]) 50[illegible]	(17.52) 17.37
B17	.0767	776.0	(516.6) 517.5	.1176	63.7	(280.4) 280.3	(473.9) 474.4	(18.01) 17.95
B18	.1164	774.7	(517.6) 517.5	.2036	62.8	(252.0) 251.8	(487.5) 488.1	(27.08) 27.08
B19	.0662	947.1	(630.5) 632.5	.0932	76.0	(360.0) 357.9	(570.7) 572.7	(18.71) 18.58
B20	.1520	951.4	(683.6) 683.3	.2128	71.8	(312.7) 313.2	(625.2) 624.8	(36.23) 36.26
B21	.1147	941.3	(607.9) 611.1	.2143	72.3	(297.8) 296.0	(587.9) 590.4	(34.16) 33.82
B22	.0754	964.4	(496.4) 501.3	.2160	73.1	(280.4) 278.8	(543.3) 546.8	(31.65) 31.31
rms error	--	--	0.40	--	--	0.31	0.34	0.03

[a] Air flow rates were determined in Reference 7 by a heat balance assuming no heat loss to the environment.

$$\text{sodium} \begin{Bmatrix} C_p = 0.3087 \text{ Btu/lbm - } ^oF \\ \dot{m} = 0.1163 \times 10^7 \text{ lbm/hr} \\ \xi = 0.5220 \\ UA = 0.1868 \times 10^6 \text{ Btu/hr - } ^oF \end{Bmatrix} \quad (10)$$

The numbers in parentheses in Table 1 are the predicted results. The root-mean-square (rms) errors in predicted outlet temperatures and the log-mean-temperature difference is no more than 0.4 ^oF. The rms error in the predicted heat transfer is 0.03 MWt (0.1% of rated power). This agreement is caused by selecting a reference state, B15, given by experiment and by choosing the 0.70 power of the Reynolds as the Nusselt number correlation.

Perkins et al.,[13] have suggested for the FFTF/DHX a Nusselt number correlation using a 0.667 power of the Reynolds number in agreement with Briggs and Young data for staggered, finned tubes.[15] In Figure 3, we find that the measured heat transfer ratios are best correlated by a Nusselt number proportional to the 0.70 power of the Reynolds number. The coefficient of determination r^2, between the prediction and the data is

$$r^2 = 0.99 \quad (11)$$

for both curves, showing that the model is accurate for forced convection flow between 0.45 and 1.1 times the reference state air flow rate.

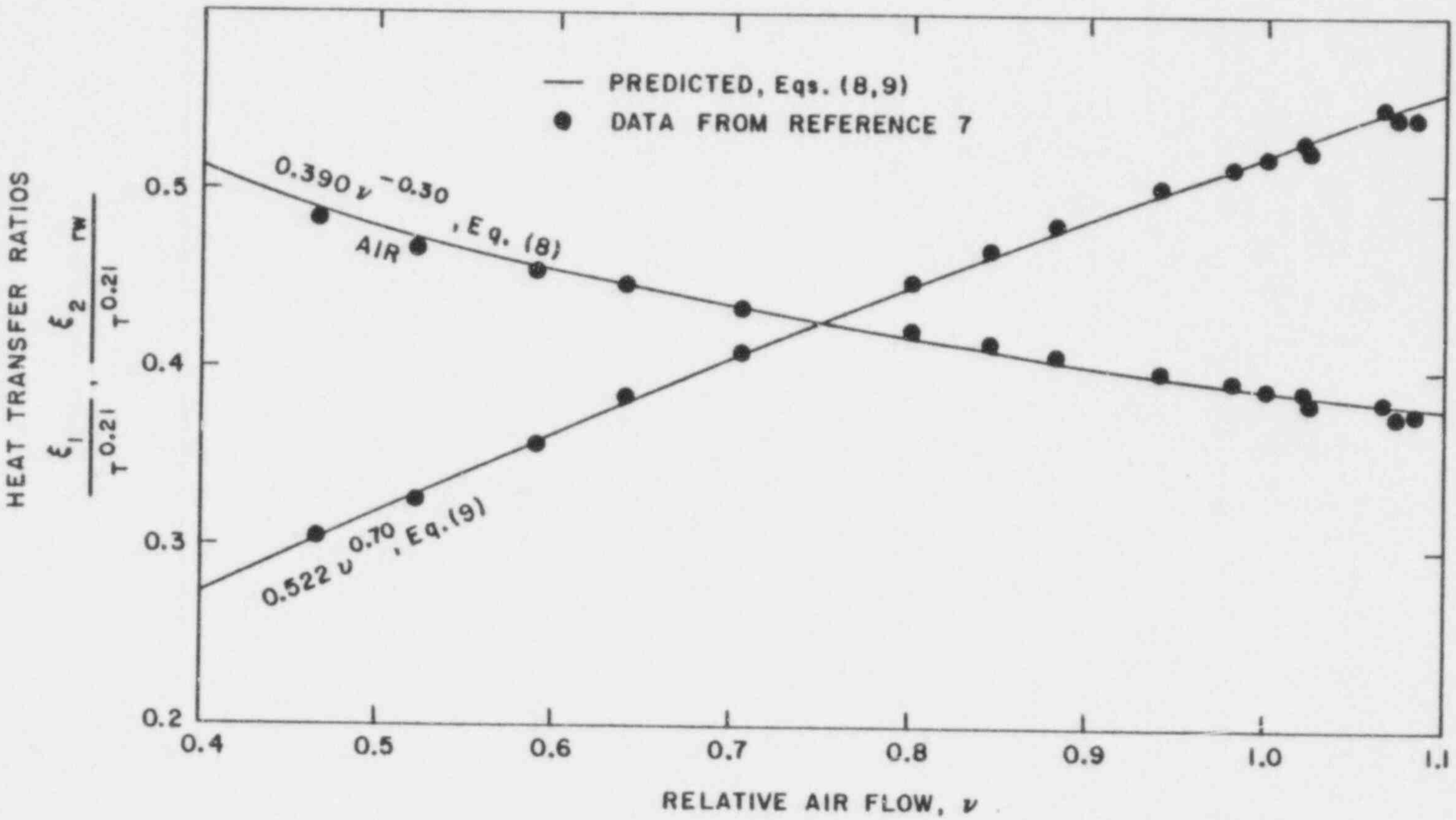

Figure 3. Heat Transfer Ratios

516 077

4. STACK BUOYANCY MODEL

Figure 4 shows the air side of the DHX.

Using a perfect gas model for air and a complete mixing model for the stack, we obtain

$$\frac{dT}{dt} = \frac{\nu}{\tau} (T_1 - T) \ {}^{o}F/sec. \ , \qquad (12)$$

$$\tau = \frac{T + 459.7}{T_o + 459.7} \tau_o \ sec. \ , \text{ and} \qquad (13)$$

$$\Delta P = 7.64 \ H \left(\frac{1}{T_o + 459.7} - \frac{1}{T + 459.7} \right) \text{ in. } H_2O \ , \qquad (14)$$

where the time constant τ_o for the stack is the stack volume divided by a reference volumetric flow rate, and H is the effective stack height in feet.

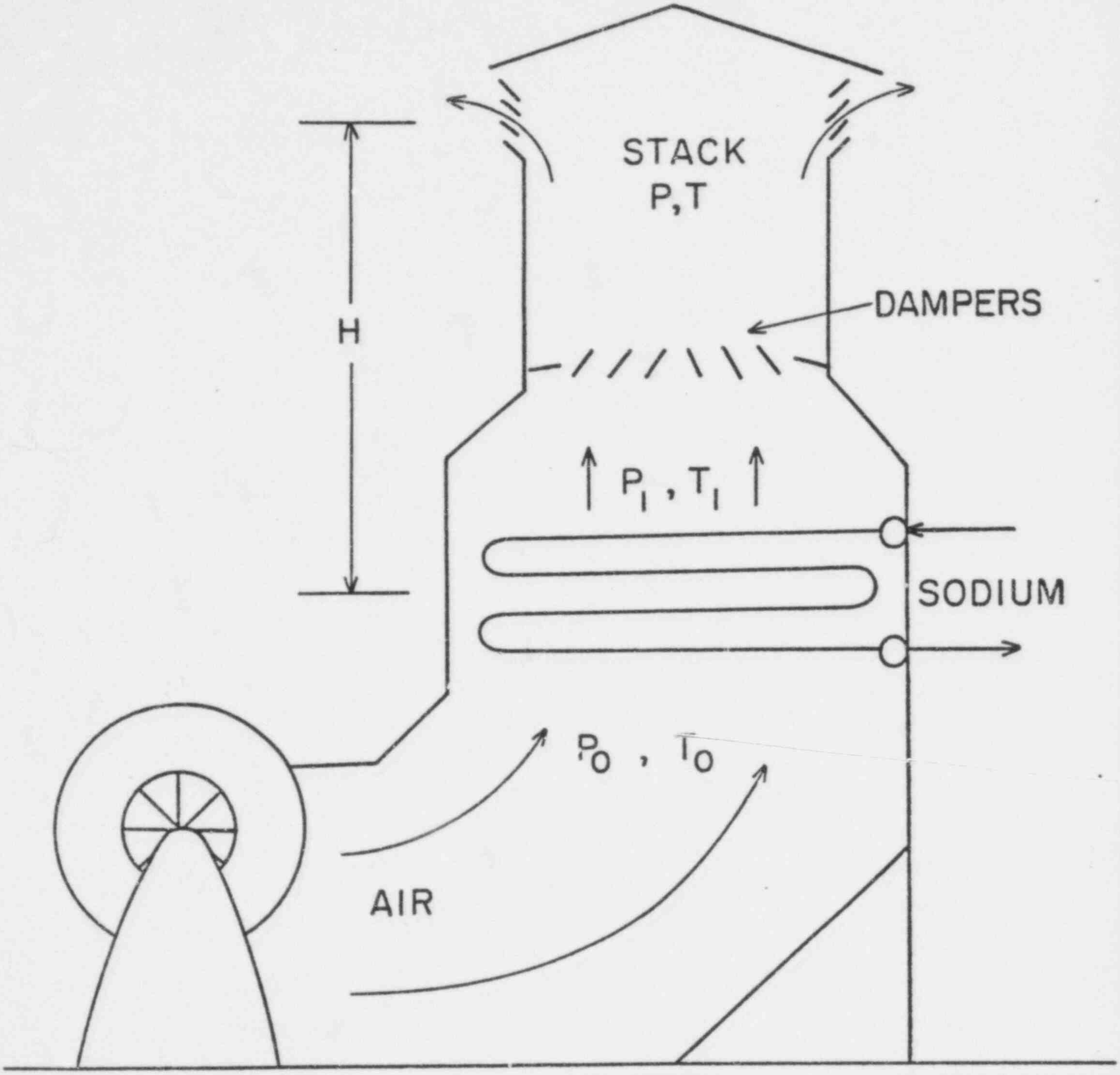

Figure 4. DHX Stack

516 079

5. CONTROL SYSTEM MODEL

The operator selects a remote set-point temperature, T_s, representing the desired sodium outlet temperature.[6] He also selects temperature offsets, ΔT_u and ΔT_M, of approximately 5^oF.[6] A set-point generator then determines a unit set-point temperature

$$T_u = T_s + \Delta T_u , \tag{15}$$

and a module set-point temperature

$$T_M = T_s - \Delta T_M . \tag{16}$$

These set-points are provided to the unit and module controllers. The purpose of the set-points is to allow automatic transfer from unit control (fan speed) to module control (damper position) without hunting between the two control modes.

The unit controller takes the unit set-point and compares it to the measured sodium outlet temperature with a measurement time delay. The resulting temperature error drives a proportional, integral, derivative controller.

The output of the controller is a demanded fan speed limited between operator set minimum and maximum fan speeds. There are field adjustable control variables: the gain, the integral repetition rate, and the derivative time. Appendix A summarizes the equations and parameters chosen for the unit controller. The same demanded fan speed is used for each of the four DHX's attached to one loop of the FFTF.[6] The unit controller integral has roll-up and roll-down limits.

A single DHX module (four per loop) has a set-point temperature a few degrees below the remote set point; see Equation (16). The sodium outlet temperature from a module is compared to this set point and the error drives a proportional, integral, derivative module controller. The output of the module controller is a demanded damper position which activates the fine and coarse damper drives. The module controller is similar to the unit controller and its parameters are listed in Appendix A.

A final function of the control system is to close and open the fan circuit breakers. If the dampers are closed and the module control system is calling for them to close even further, the fan breaker is opened. Similarly, if the dampers are open and the module controller demands greater flow, the fan breaker is closed. This function of the control system is not discussed in the system design description,[6] but is included here to make the model more complete. This feature of the system code implies that all four modules per loop are in operation at the same conditions.

6. MOTOR AND MAGNETIC DRIVE MODEL

The magnetic drive exciter is a solid state device utilizing a silicon-controlled-rectifier to supply d-c excitation current to the collector rings of the rotating magnet coil of the magnetic drive.(5) We model the time behavior of the excitation current I, normalized to its maximum value, as

$$\frac{dI}{dt} = \frac{1}{\tau} (\alpha_d - \alpha) \quad , \tag{17}$$

where

$$0 \leq I \leq 1 \quad . \tag{18}$$

The number, $\alpha_d - \alpha$, is the difference between the demanded fan speed from the unit controller and the actual fan speed measured by a tachometer attached to the fan shaft. The quantity τ is a time constant of the order of 10^{-4} seconds. This makes the response speed very fast resulting in I being 0 or 1 for all but minute speed errors. The exciter, therefore, acts as a Bang-Bang controller.

The unit controller coupled through the exciter to the magnetic drive provides a high gain unstable feedback system. The instability is limited in magnitude by the exciter output current. This results in the fan speed fluctuating slightly as the exciter activates and deactivates the magnetic coupling. This is a usual feature of variable-speed magnetic drives.(5)

The eddy-current magnetic drive has an outer rotating steel ring driven by the fan motor. A rotating magnetic coil attached to the fan is driven by magnetic fields and resulting eddy currents in the rotating ring. The magnet coil is excited by a d-c current supplied through collector rings. The transmitted torque is determined by the exciter current and the relative speed of the ring and magnet coil. We approximate the torque $\beta_C(\Delta S, I)$ by

$$\beta_C(\Delta S, I) = \frac{K\,\Delta S\,(2\sigma + A)}{(\Delta S)^2 + A\,\Delta S + \sigma^2}\ , \tag{19}$$

where K, σ, and A are functions of the exciter current, I. In Equation (19) ΔS is the relative slip, K is the maximum torque, σ is the value of the relative slip resulting in the maximum torque, and A is a current dependent parameter. Figure 5 shows values of β_C as a function of relative slip and current.

The motor torque is modeled by a well known equivalent circuit for a poly-phase induction motor. This is due to Steinmetz[11] and is discussed by Kron[10] and Fitzgerald and Kingsley.[9] The resulting expression for the motor torque is

$$\beta_M = \frac{A\,r_2/S}{(R_1 + r_2/S)^2 + X^2}\ , \tag{20}$$

where R_1 is the stator resistance, r_2 is the rotor resistance, X is the mutual inductance, and S is the motor slip. We alter the parameters slightly to get the equivalent equation

$$\beta_M(S) = \frac{K_r S\,(2S_0 + a)}{S^2 + aS + S_0^{\,2}} \tag{21}$$

where the parameters are based on Reference 8, 18 and are given in Appendix A. Figure 6 shows the resulting motor torque. We assume that the motor has a very small moment of inertia and can immediately adjust its speed. This amounts to the simultaneous solution of the equation matching the motor and magnetic drive torques, Equation (19) and (21);

$$\beta_M(S) = \beta_C(\Delta S, I) \tag{22}$$

516 083

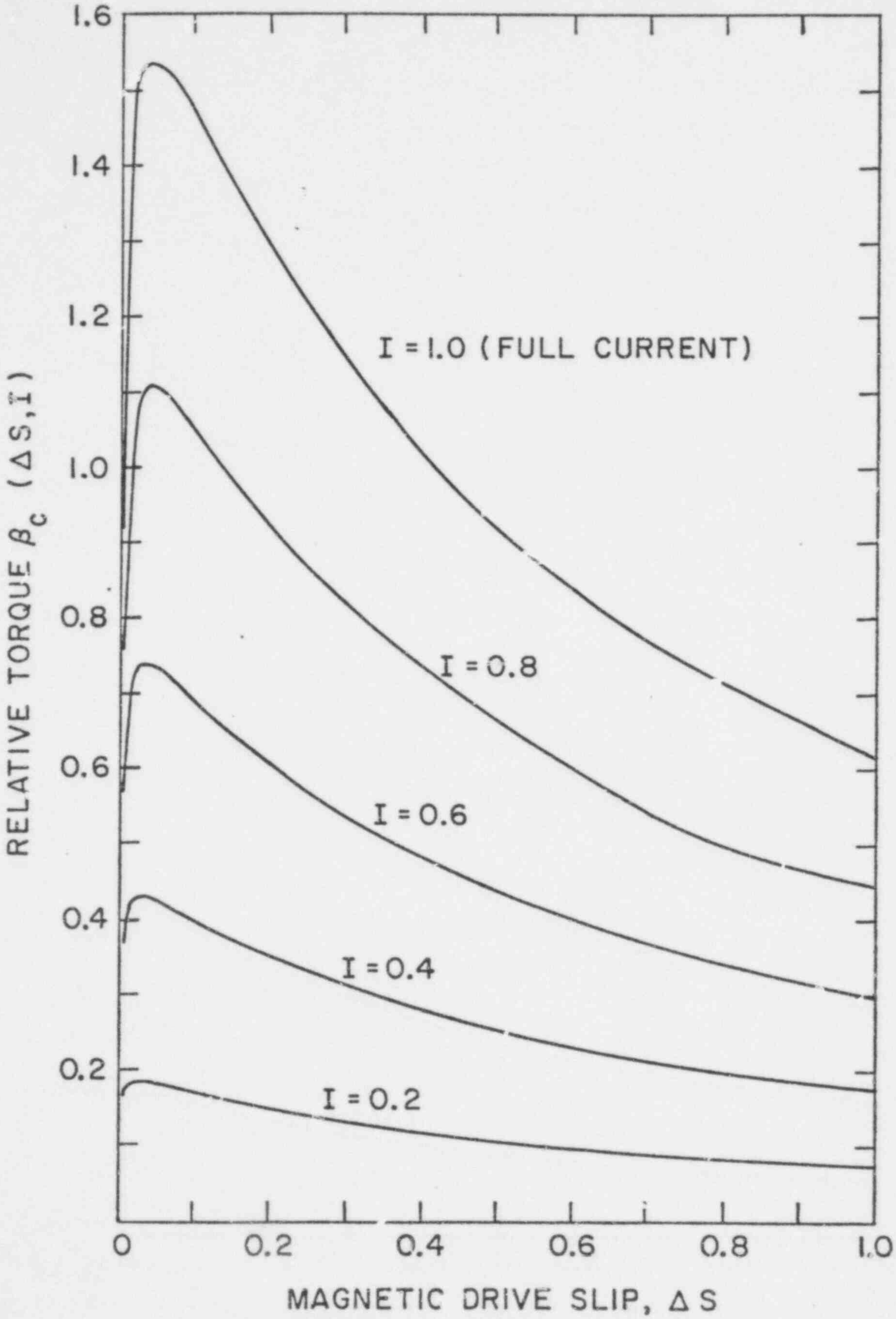

Figure 5. Magnetic Drive Torque

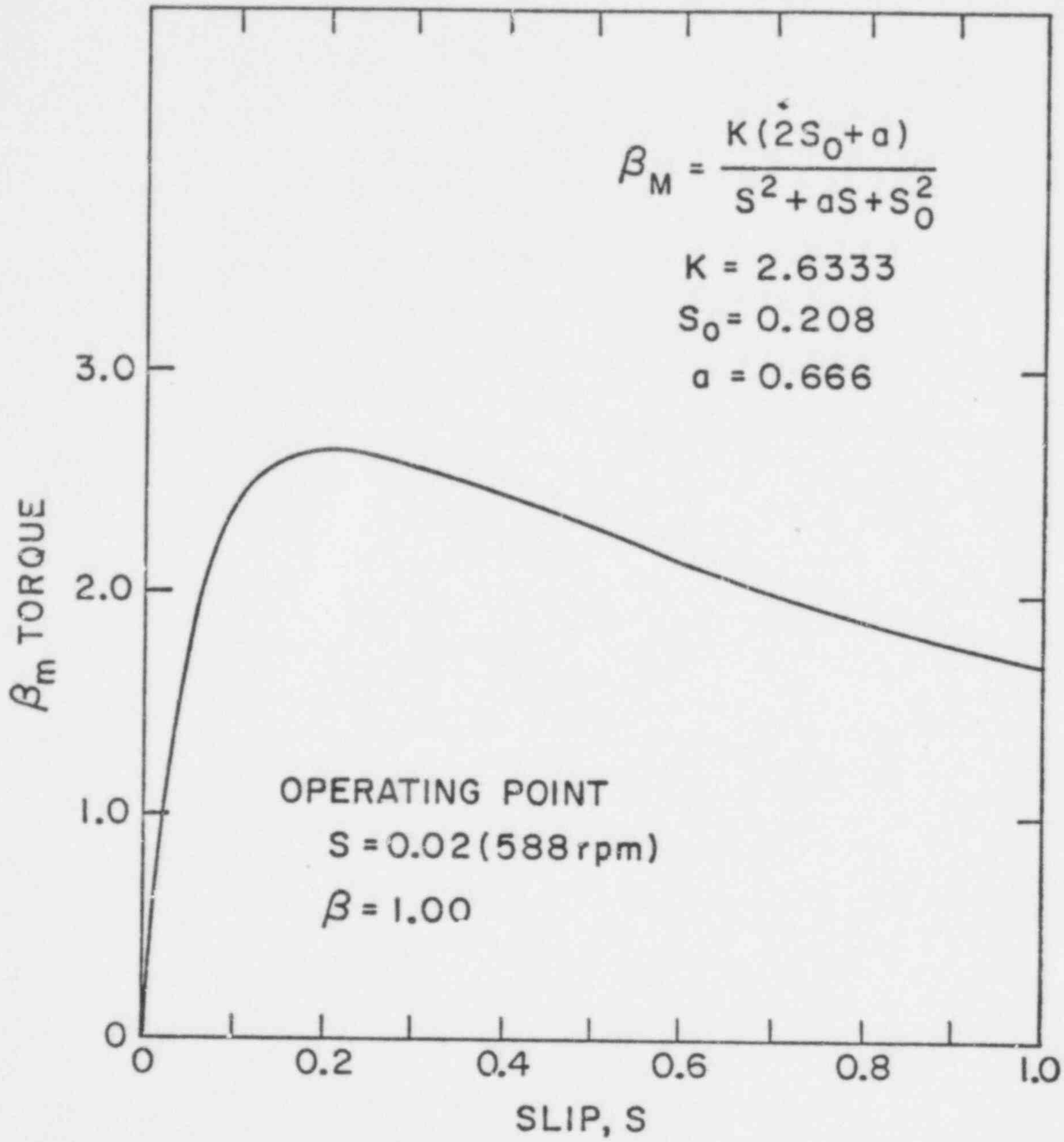

Figure 6. Motor Torque

and the following relationship between the motor slip, S, and the magnetic drive relative slip, ΔS:

$$S = 1 - \Delta S - \alpha \frac{N_r}{N_s} \quad , \qquad (23)$$

where

α is relative fan speed,

N_r = 532 rpm, the reference fan speed, and

N_s = 600 rpm, the synchronous motor speed.

Subroutine DRIV3T and DRIV3S solves Equations (22) and (23) simultaneously for a given fan speed α and exciter current I. This solution is a pair of slips S, ΔS which satisfy the two equations. In Figure 7 we plot the resulting torque as a function of fan speed and exciter current. The curve shows that the torque falls off very rapidly above $\alpha \approx 1.08$. This is the main physical limitation on the air side flow rate.

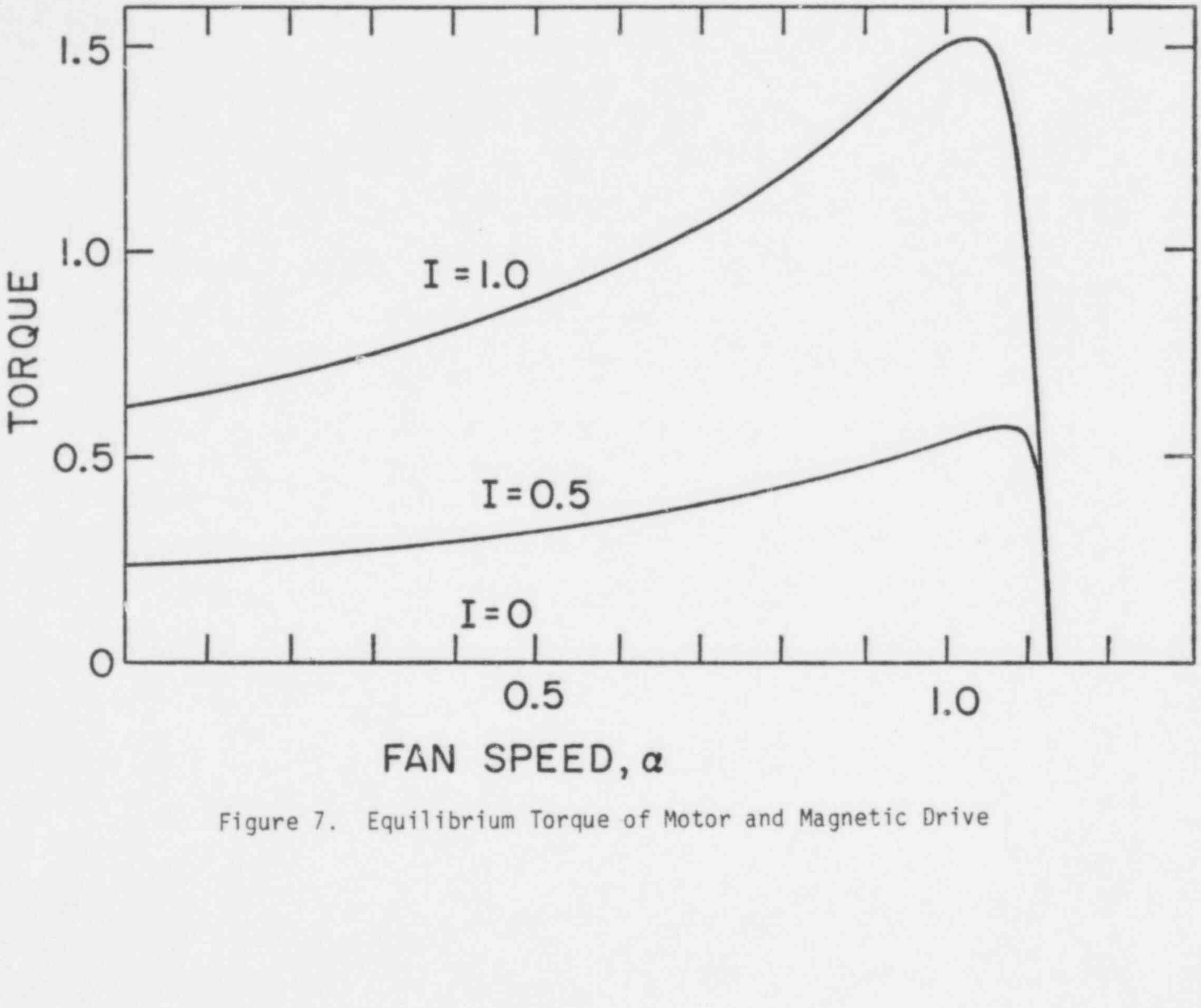

Figure 7. Equilibrium Torque of Motor and Magnetic Drive

7. FAN MODEL

The inertia of the fan and the rotating magnet is large, giving a time constant of

$$\tau = \frac{J\ 2\pi\ N}{60\ g_o\ T} = 16 \text{ sec.} , \tag{24}$$

where

J = 112,460 ft^2- lbm, moment of inertia,

N = 532 rpm, fan speed, and

T = 11,917 ft-lbf, reference fan torque.

Conservation of angular momentum gives

$$\tau \frac{d\alpha}{dt} = (\beta_c - \beta - \beta_f) , \tag{25}$$

where

β_c is the relative magnetic drive torque,

β is the fan torque, and

β_f is the frictional torque.

We model the low speed frictional torque as 4% at zero speed and decreasing linearly to zero at 6½% speed; that is

$$\beta_f = \begin{cases} 0.04\ (1 - \frac{\alpha}{0.065}), & \alpha \leq 0.065 , \\ 0, & \alpha > 0.065 . \end{cases} \tag{26}$$

This model accurately predicts measured speeds in a fan coastdown test performed March 19, 1975.[7] Figure 8 shows the comparison of the model with these experimental results.

516 088

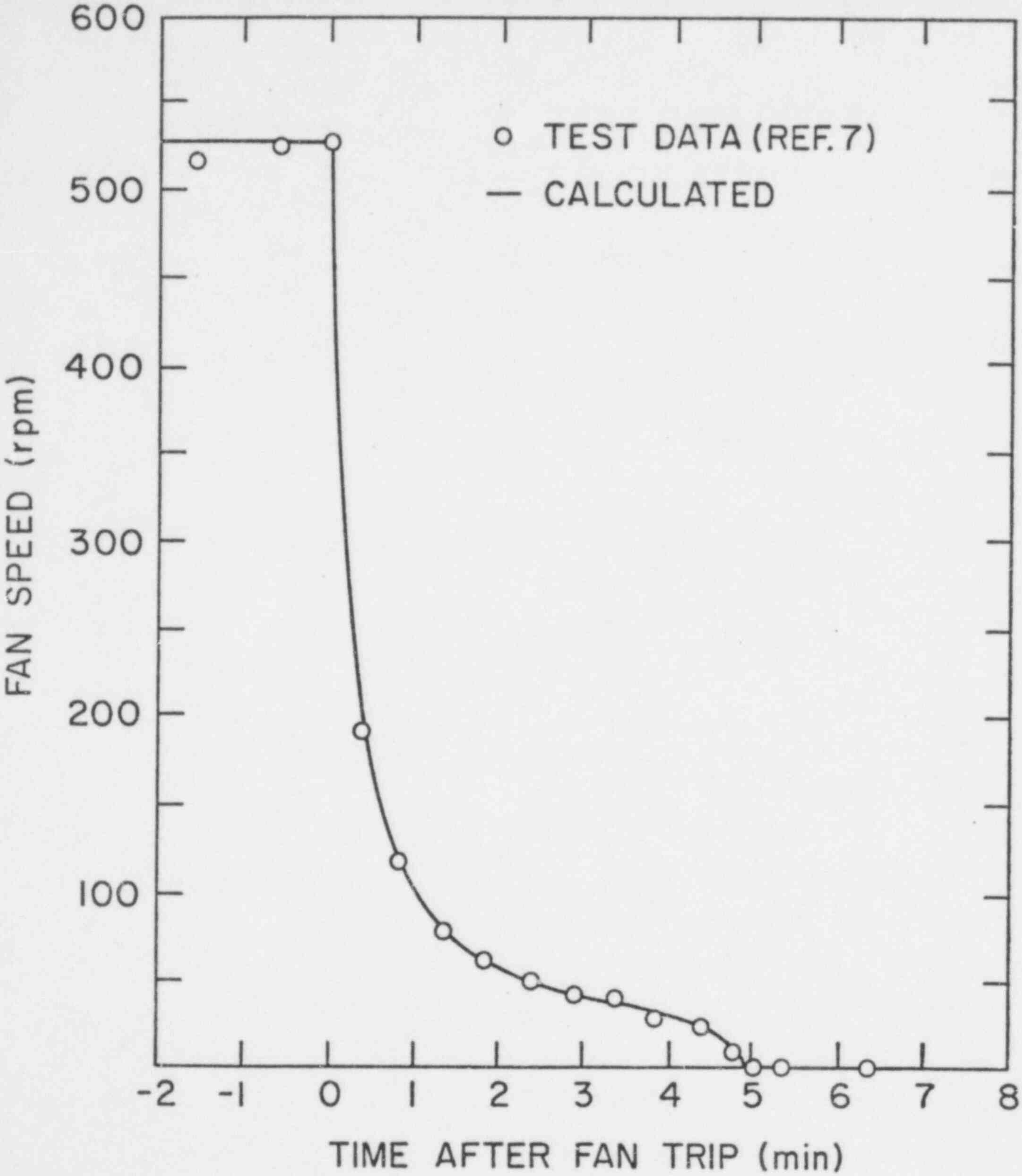

Figure 8. DHX Fan Coastdown Test

516 089

The fan head $\delta(\alpha,\nu)$ is modeled by homologous curves of the form

$$\delta = -h + \begin{cases} \alpha^2 \sum_{i=1}^{5} a_i \left(\frac{\nu}{\alpha}\right)^{i-1} \; ; & \nu \leq \alpha \\ \nu^2 \sum_{i=1}^{5} b_i \left(\frac{\alpha}{\nu}\right)^{i-1} \; ; & \alpha < \nu \end{cases} , \tag{27}$$

where the head resistance of the variable-inlet-vanes is given empirically as a function of vane angle, θ, as

$$h = \begin{cases} \left[e_1 \left(e_2^{\theta/75} - e_2\right) + e_3 \left(1 - \frac{\theta}{75}\right)\right] \nu^2 & , \; \theta \leq 75^0 \\ 0 & , \; 75^0 < \theta < 90^0 \end{cases} . \tag{28}$$

Similarly, the fan torque is given by

$$\beta = \begin{cases} \alpha^2 \sum_{i=1}^{5} c_i \left(\frac{\nu}{\alpha}\right)^{i-1} \; ; & \nu \leq \alpha \\ \nu^2 \sum_{i=1}^{5} d_i \left(\frac{\alpha}{\nu}\right)^{i-1} \; ; & \nu > \alpha \end{cases} . \tag{29}$$

The coefficients a_i, b_i, c_i, d_i, e_i, based on References 8 and 16, are given in Appendix A.

Curves of relative head δ, relative efficiency η, and relative torque β, are shown in Figures 9, 10, and 11.

Figures 12 shows contours of relative head $\delta(\alpha,\nu)$ and Figure 13 shows contours of relative torque $\beta(\alpha,\nu)$ chosen for the DHX fans.

Figure 14 shows the relative fan head as a function of flow and variable-inlet-vane angle.

516 090

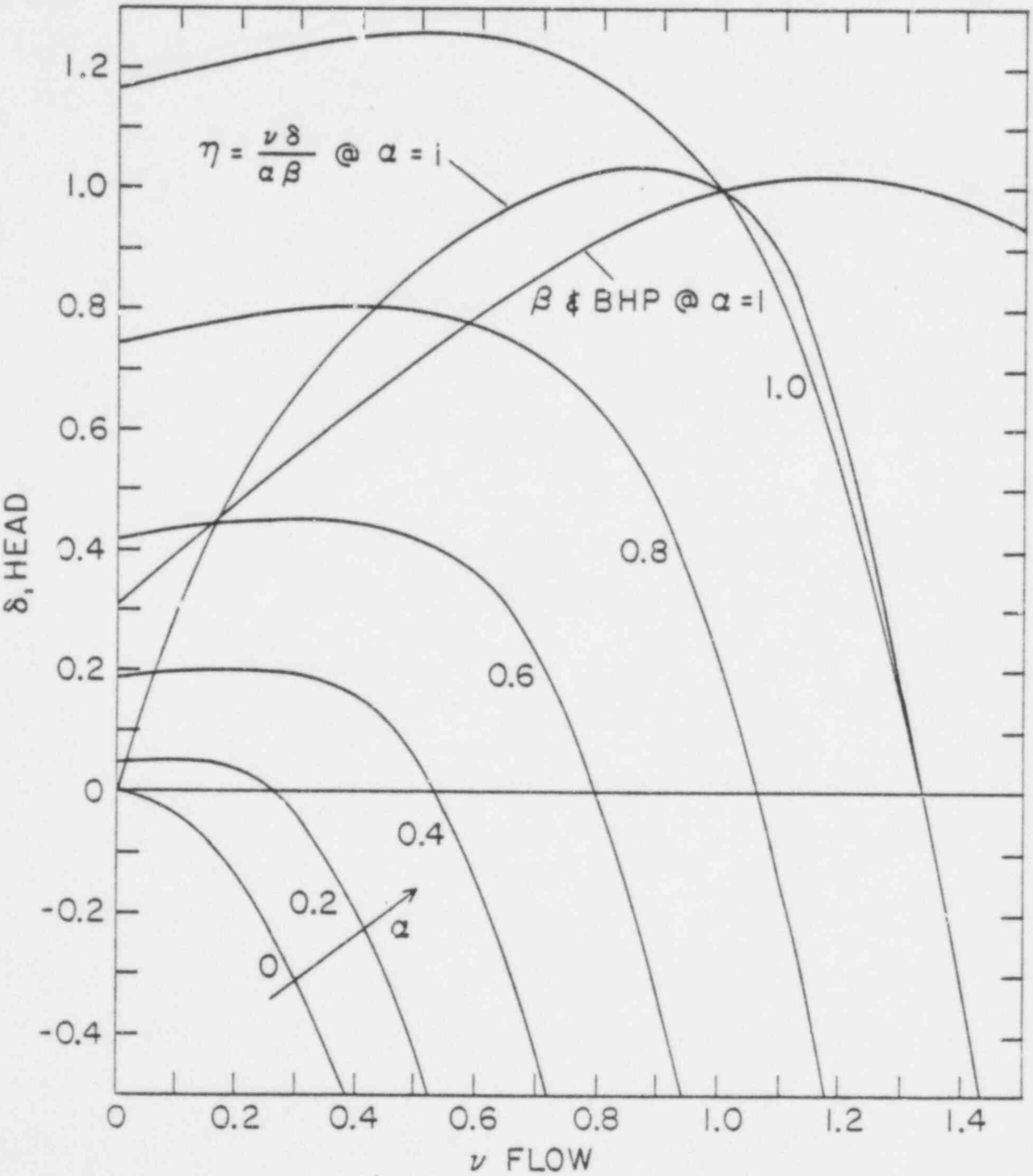

Figure 9. Head, Efficiency, and Torque

516 091

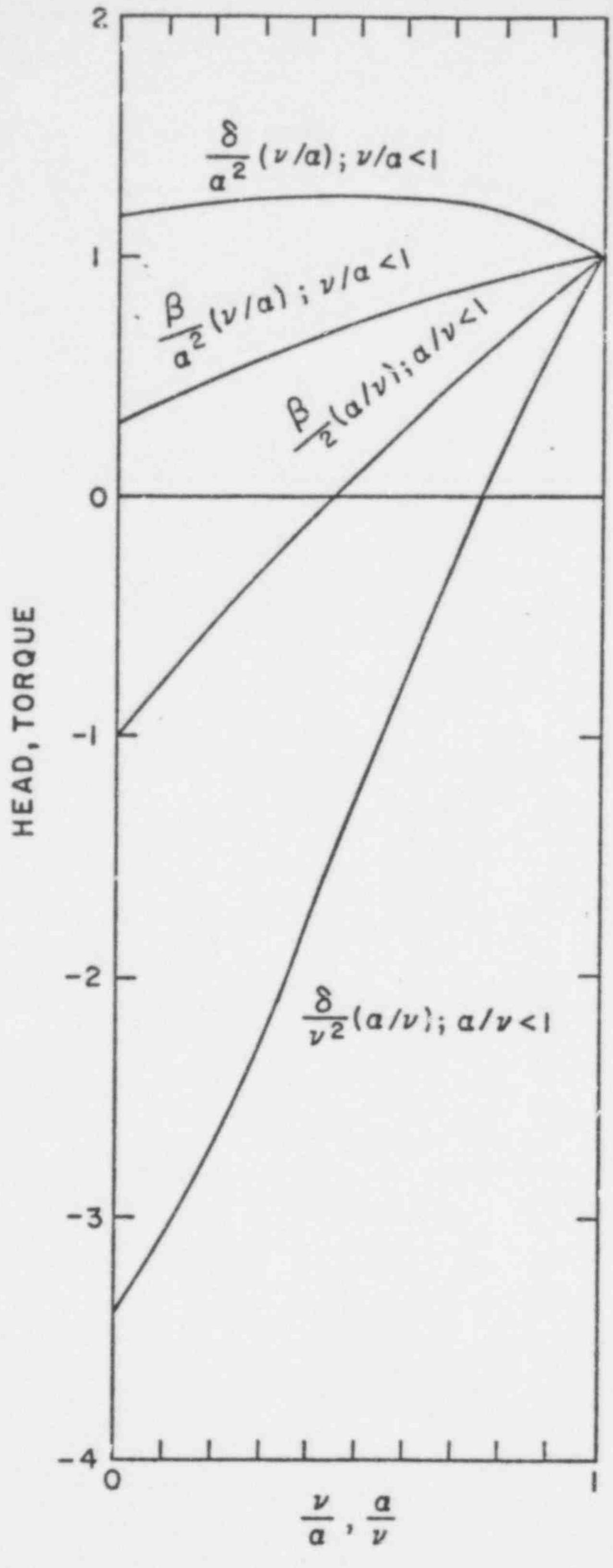

Figure 10. Head and Torque

516 092

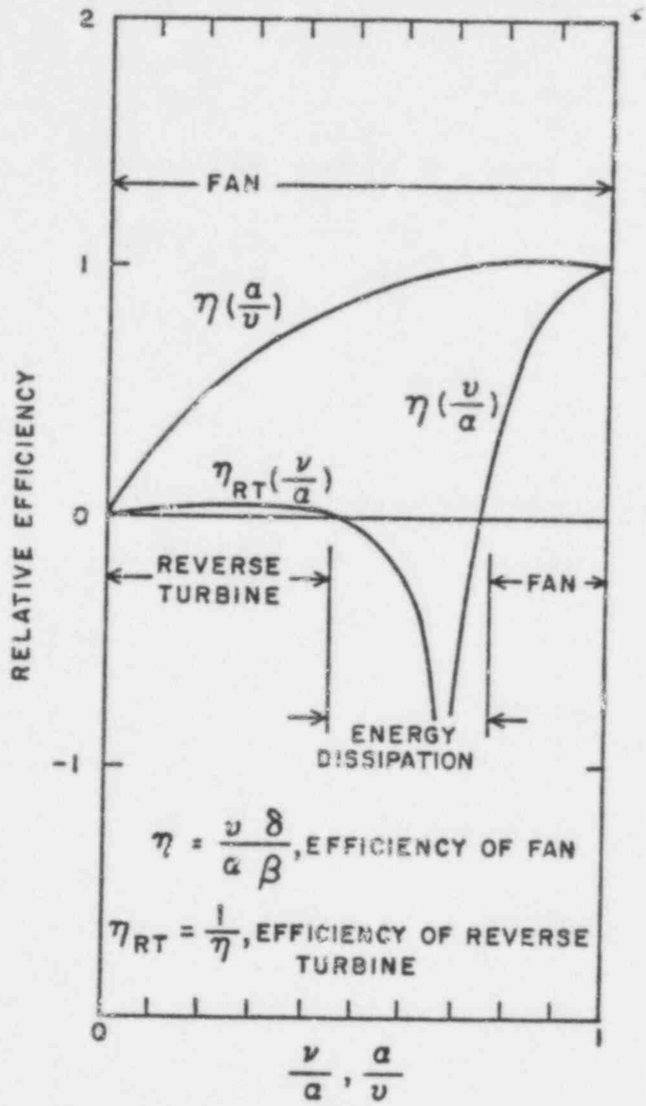

Figure 11. Relative Efficiency

516 093

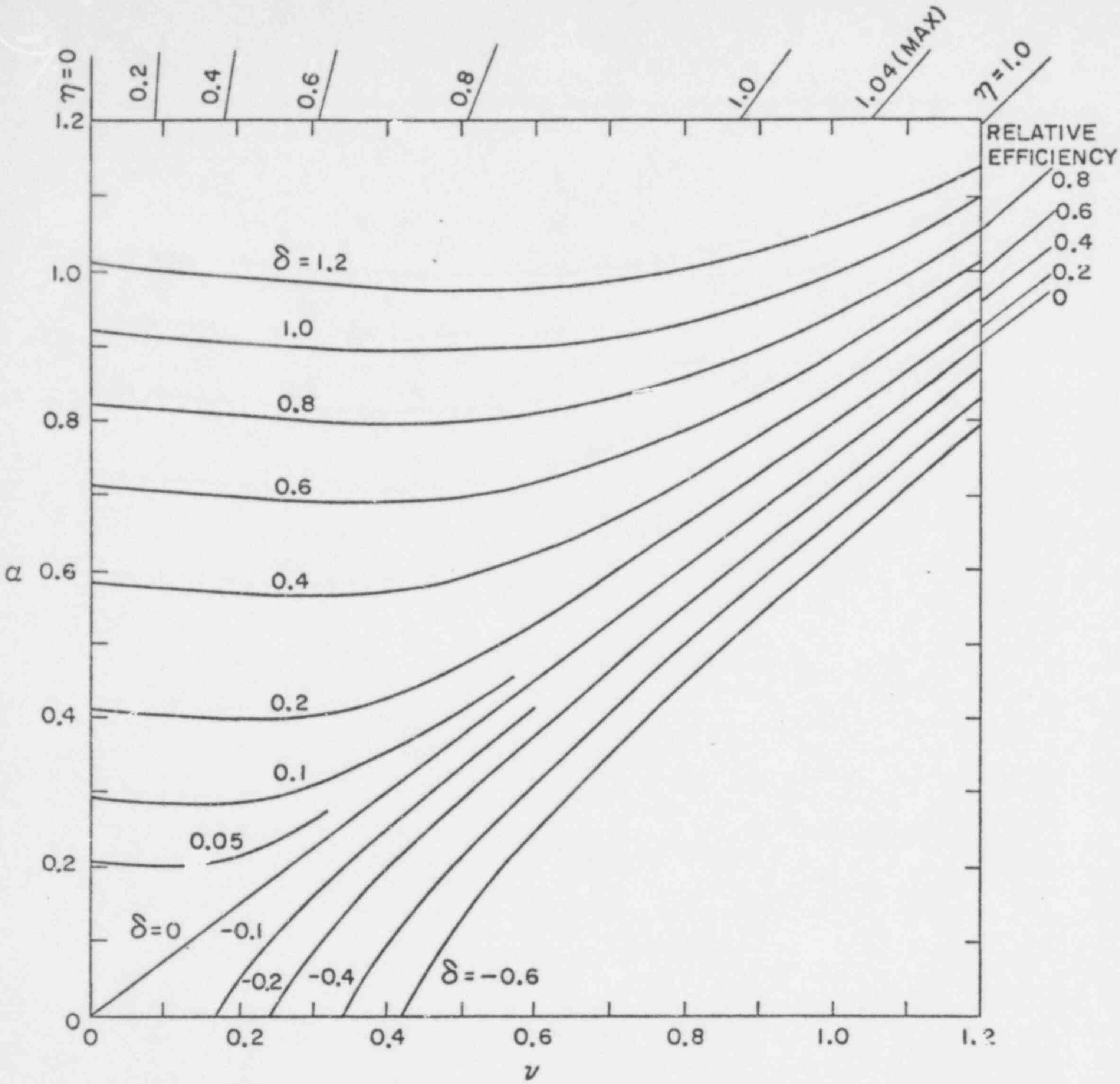

Figure 12. Head Contours

516 094

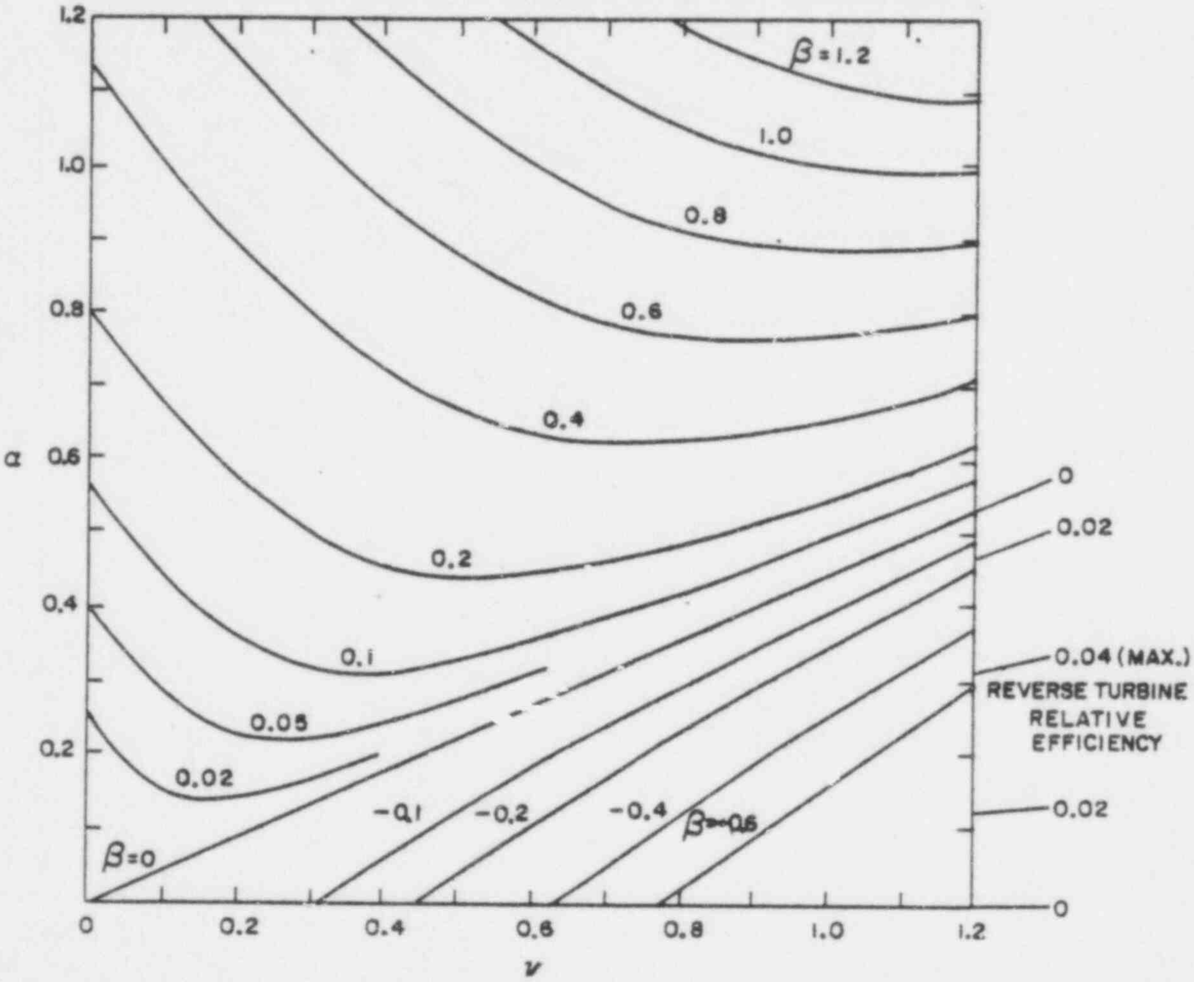

Figure 13. Torque Contours

516 095

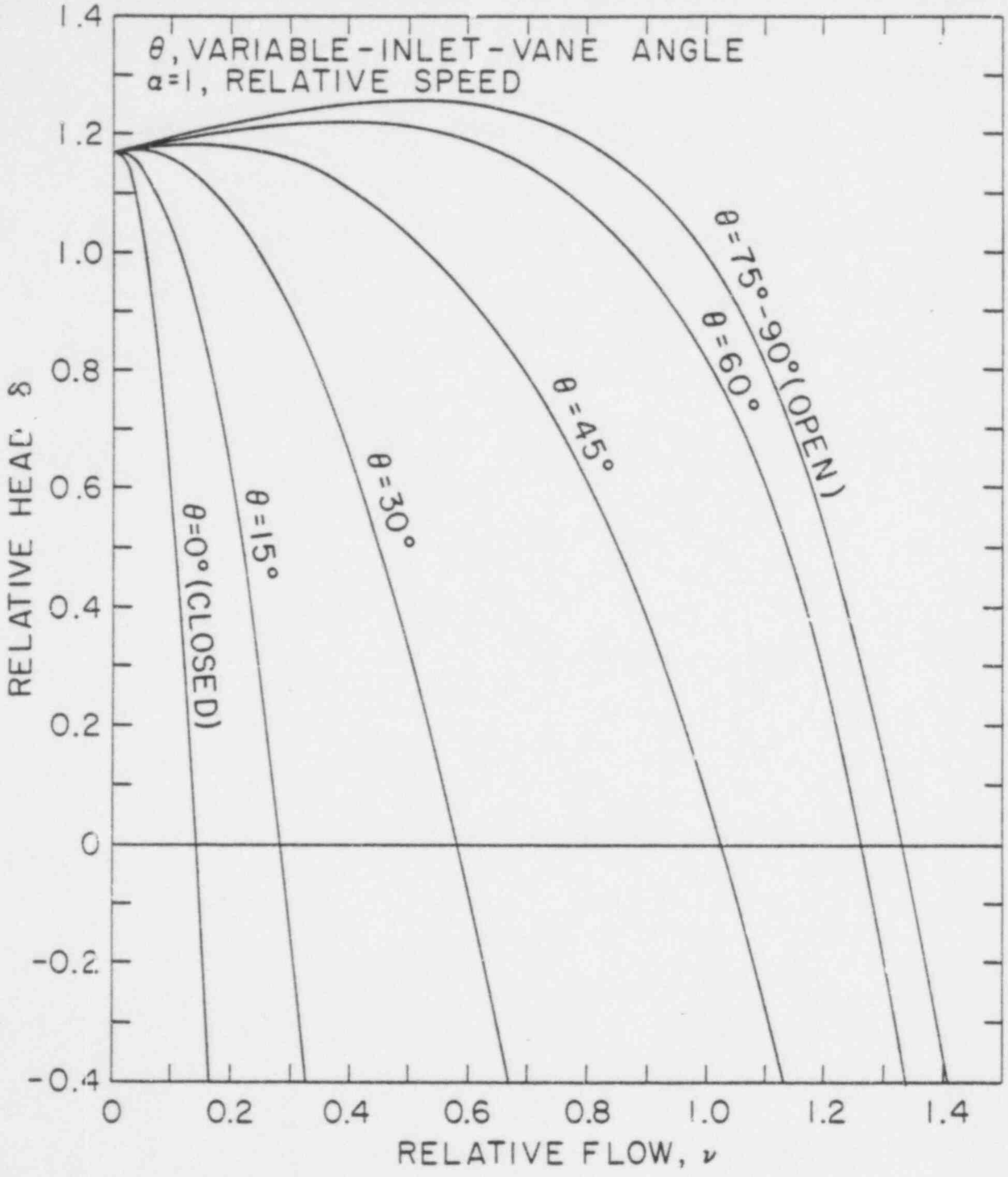

Figure 14. Fan Head vs. Flow and Vane Angle

516 096

The air flow across the heated, finned tubes is modeled assuming the following:

1) air is a perfect gas,

2) we have a steady flow process; i.e., no air inertia,

3) there is a constant flow area through the tube bundles,

4) there is a polytropic process between absolute pressure P_1 and absolute temperature T_1 at the fan outlet to absolute pressure P_2 and absolute temperature T_2 at the exit from the tube bundle.

The following momentum balance is used:[3]

$$vdP + \frac{g}{g_o}\,dz + \frac{G^2 v dv}{g_o} + \frac{2\,fG^2 v^2}{g_o D}\,dx = 0\ , \qquad (30)$$

where

v is the specific volume,

P is the absolute pressure,

z is the height,

G is the mass velocity,

g is the acceleration of gravity,

g_o is a conversion factor,

D is the effective hydraulic diamete

f is the Fanning friction factor, and

x is distance through the bundle.

Dividing by v^2 and integrating between the inlet to the tube bundle, state 1, and the outlet from the tube bundle, state 2, gives

$$\int_{P_1}^{P_2} \frac{dP}{v} + \frac{g}{g_o}\int_{z_1}^{z_2} \frac{dz}{v^2} + \frac{G^2}{g_o}\int_{v_1}^{v_2} \frac{dv}{v} + \frac{2\,fG^2}{g_o D}\int_{x_1}^{x_2} dx = 0\ . \qquad (31)$$

In order to perform these integrations we take the assumed polytropic process between P_1, T_1, and P_2, T_2,

$$Pv^{\alpha} = C \, , \tag{32}$$

the assumed perfect gas model,

$$Pv = RT \, , \tag{33}$$

and we neglect the gravity term. This results in the following equation:

$$g_o \frac{P_1}{v_1} \left(1 - \frac{1}{r^2 t}\right) \left(\frac{1}{1 + \frac{\ell n(rt)}{\ell n(r)}}\right) = G^2 \left(\ell n(rt) + \frac{K}{2}\right) \, , \tag{34}$$

where we have defined

$r = P_1/P_2$, the absolute pressure ratio,

$t = \frac{T_2}{T_1}$, the absolute temperature ratio, and

$K = \frac{4fL}{D}$, the tube bundle drag coefficient.

We choose reference values for each variable in Equation (34) except K which is determined by the equation itself. Appendix A lists the parameters and reference values chosen; which result in a reference value K_r of 8.260 velocity heads with the dampers open.

Perkins et al.,[13] have suggested a drag coefficient across the finned tubes of the FFTF/DHX proportional to the 0.316 power of the Reynolds number based on the work of Robinson and Briggs,[14] for both staggered and unstaggered finned tube bundles. Using a viscosity dependence of air on temperature given by Equation (3) and assuming the same drag behavior for the dampers, we add to K_r the drag coefficient of the dampers K_d to obtain,

$$\overline{K} = (K_r + K_d) \, \nu^{-0.32} \left(\frac{T_2}{T_{2r}}\right)^{0.23} \, , \tag{35}$$

516 098

where ν is the relative air mass flow rate, and T_1/T_{2r} is the outlet air absolute temperature ratio.

In order to use Equation (34) for other than the reference air flow conditions, we change G to $G\nu$ and K to $\overline{K}$ and solve for ν,

$$\nu = \left[\left(\frac{g_0}{RG^2} \right) \frac{P_1{}^2}{T_1} \; \frac{\left(1 - \frac{1}{r^2 t} \right)}{\left(1 + \frac{\ln(rt)}{\ln(r)} \right) \left(\ln(rt) + \frac{\overline{K}}{2} \right)} \right]^{1/2} , \qquad (36)$$

as the system head curve relating the flow ν with the driving head appearing in the pressure ratio r. The simultaneous solution of Equation (36) with the fan head curve Equation (27) determines head and flow for a given fan speed α and damper and vane positions.

516 099

8. OUTLET DAMPER MODEL

The outlet dampers are driven by a constant speed sequential drive. The fine dampers are opened before the coarse dampers and the coarse dampers are closed before the fine dampers close.[6] Figure 15 shows the eight damper model used in DHX3T and DHX3S. Two dampers constitute the fine dampers and the other six are the coarse dampers. References 6, 8, and 17 discuss the FFTF/DHX stack dampers.

The damper signal, χ, from the module controller is converted into a demanded position for both the fine and coarse dampers. If their actual position is different from the demanded position the dampers are driven open or closed with a constant speed. The equations appear in Appendix A.

When both dampers are closed the flow area is reduced to $a = 0.05$ of the fully opened dampers. We use a single orifice model[3] to predict the drag coefficient of the partially opened dampers:

$$K_d = \left[\frac{1}{1 - \frac{6}{8}\,(1 - a)\cos\left(\frac{\chi_c \pi}{2}\right) - \frac{2}{8}\,(1 - a)\cos\left(\frac{\chi_f \pi}{2}\right)}\right]^2 - 1 \,, \qquad (37)$$

The drag coefficient is zero for fully opened dampers, $\chi_c = \chi_f = 1$, and is 399 for fully closed dampers, $\chi_f = \chi_c = 0$.

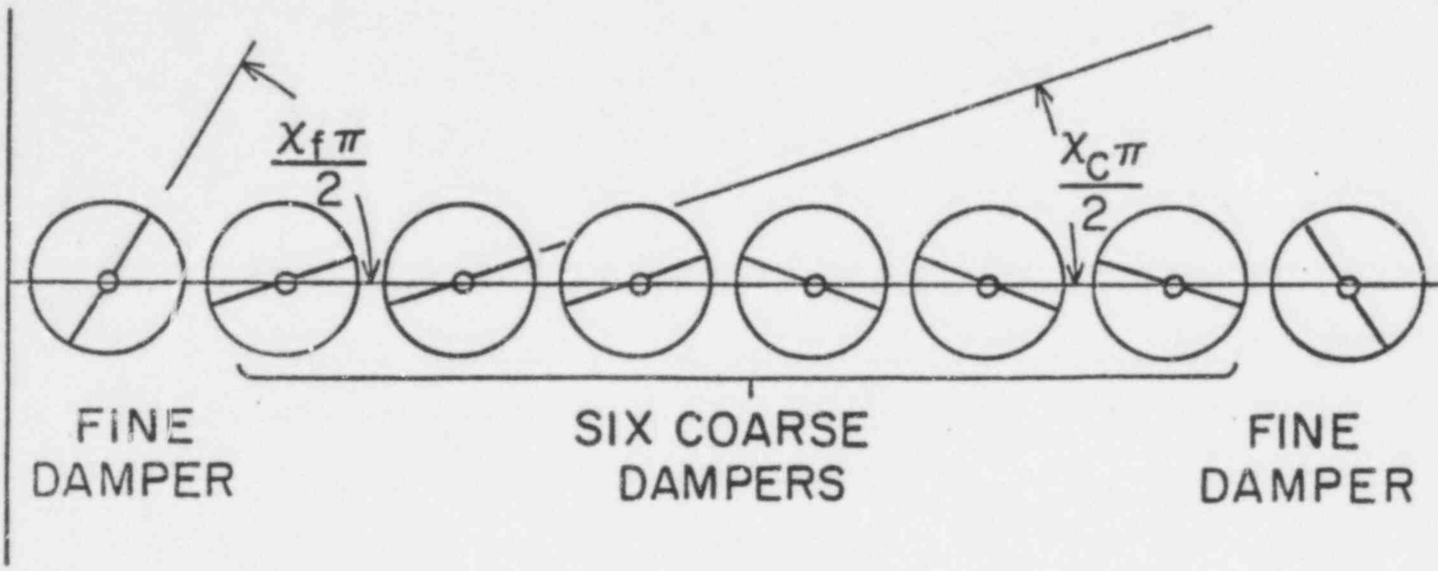

Figure 15. Fine and Coarse Dampers

516 101

9. STEADY STATE FORCED CONVECTION, COMPARISON OF MODEL WITH TEST RESULTS

The DHX system code has a steady state version, DHX3S, which can be used to predict steady state operating conditions as a function of

1) sodium flow,
2) inlet sodium temperature,
3) inlet air temperature,
4) remote set-point temperature,
5) variable inlet vane angle, and
6) fan breaker open/closed.

We have compared the results with eighteen steady state forced convection tests.[7] These comparisons verify the approximate accuracy of

1) the head and torque characteristic curves for the fans,
2) the natural convection driving buoyancy,
3) the tube bundle air side flow resistance, and
4) the variable inlet vane flow resistances.

Table 2 shows the eighteen steady state forced convection predictions compared with measured results. For this comparison we have set the remote set-point to give the measured outlet sodium temperatures and have compared the predicted results for

1) air outlet temperature,
2) log mean temperature difference,
3) fan speed, and
4) air flow rate

TABLE 2

As Built FFTF HTS/DHX Steady-State Test Data June 16-21, 1975[7] (Cont.)

	Specified Conditions					Comparison of Measured Results and Predicted Results (in parentheses)				
Page (Ref.7)	inlet vane angle °F	sodium flow rate 10 lbm/hr	inlet sodium temp. °F	outlet sodium temp. °F	heat transferred MWt	relative air flow 1.995 x 10 lbm/hr	outlet air temp. °F	log mean temp. diff. °F	fan speed RPM	relative fan speed 532 RPM
B4	53.7	1.168	688.9	519.5	17.92	(0.645) 0.640	(256.3) 257.7	(446.4) 445.6	(391) 376.5	(.736) .708
B5	53.8	1.169	688.7	519.4	18.00	(0.643) 0.640	(254.1) 255.2	(449.4) 448.8	(389) 373.5	(.732) .702
B6	53.8	1.169	688.9	519.2	18.04	(0.644) 0.640	(253.5) 254.7	(450.2) 449.5	(390) 372.0	(.732) .699
B7	54.2	1.173	703.8	519.3	19.66	(0.710) 0.704	(251.5) 253.1	(458.7) 457.9	(425) 408.1	(.798) .767
B8	54.0	1.170	724.1	519.1	21.76	(0.811) 0.801	(256.0) 258.5	(461.0) 459.8	(484) 478.9	(.909) .900
B9	54.0	1.168	735.4	519.1	27.91	(0.857) 0.846	(255.3) 257.8	(467.0) 465.7	(509) 507.7	(.956) .954
B10	54.0	1.168	744.8	519.3	23.87	(0.893) 0.883	(254.3) 256.6	(472.6) 471.5	(529) 531.0	(.994) .998
B11	53.9	1.167	760.1	519.0	25.36	(0.950) 0.941	(253.5) 255.5	(481.1) 480.1	(560) 568.1	(1.053) 1.068
B13	58.4	1.162	772.0	519.2	26.59	(0.984) 0.982	(284.0) 248.5	(493.1) 492.9	(554) 563.2	(1.042) 1.059

516 103

TABLE 2 (Cont.)

Page (Ref.7)	inlet vane angle °F	sodium flow rate 10 lbm/hr	inlet sodium temp. °F	outlet sodium temp. °F	heat transferred MWt	relative air flow 1.995×10^6 lbm/hr	outlet air temp. °F	log mean temp. diff. RPM	fan speed RPM	relative fan speed 532 RPM
	Specified Conditions					Comparison of Measured Results and Predicted Results (in parentheses)				
B14	78.9	1.175	765.7	518.3	26.32	(1.014) 1.023	(257.7) 256.2	(475.9) 476.6	(538) 556.8	(1.012) 1.047
B15	78.9	1.163	771.3	521.7	26.27	(1.000) 1.000	(259.7) 259.7	(479.6) 479.6	(532) 533.4	(1.000) 1.003
B16	57.8	0.758	816.9	562.4	17.37	(0.517) 0.522	(309.6) 306.9	(499.7) 501.0	(314) 308.8	(.590) .580
B17	57.8	0.767	776.0	517.5	17.95	(0.589) 0.589	(280.9) 280.3	(474.2) 474.4	(350) 346.8	(.659) .652
B18	67.3	1.164	774.7	517.5	27.08	(1.024) 1.021	(251.3) 251.8	(488.3) 488.1	(551) 561.5	(1.036) 1.055
B19	55.3	0.662	947.1	632.5	18.58	(0.465) 0.467	(361.0) 357.9	(571.2) 372.7	(295) 282.4	(.554) .531
B20	77.3	1.520	951.4	683.3	36.26	(1.073) 1.067	(312.5) 313.[illegible]	(625.1) 624.8	(578) 565.5	(1.087) 1.063
B21	75.4	1.147	941.3	611.1	33.82	(1.060) 1.074	(299.4) 296.0	(588.9) 590.4	(569) 580.5	(1.070) 1.091
B22	83.8	0.754	964.4	501.3	31.31	(1.064) 1.083	(282.6) 278.8	(545.2) 546.8	(568) 579.2	(1.067) 1.089
rms error						(.008)	(2.0)	(1.0)	(11.3)	(.021)

516 104

with the measured results. The predicted values are in parentheses. The rms (root-mean-square) errors for the air flow are less than 1% of the full air flow, the outlet air temperature rms error is $2^{O}F$, the log mean temperature difference rms error is $1^{O}F$, and the fan speed rms error is 11 rpm (2% of rated speed).

10. STEADY STATE NATURAL CONVECTION

COMPARISON OF MODEL WITH TEST RESULTS

We have compared predicted results with four high sodium flow natural convection tests and one low sodium flow natural convection test.[7] Table 3 shows these comparisons. Under natural circulation conditions, the prototype DHX measurements showed a maximum of 2.25 MWt transferred under both low and high flow sodium conditions. The agreement of the predicted power with measured power is good; the rms error for the five runs is 0.11 MWt.

TABLE 3

Natural Circulation Steady-State DHX Performance

Inlet Conditions				Predicted Results					Measured Results
variable inlet vane angle o	sodium flow 10^6 lbm/hr	inlet sodium temp. ^oF	air inlet temp. ^oF	sodium outlet temp. ^oF	air outlet temp. ^oF	log mean temp. diff. ^oF	relative air flow 1.995×10^6 lbm/hr	Power MWt	Measured Power MWt
7^o	1.072	528.0	70.0	515.9	383.7	267.3	0.0271	1.20	1.26
17^o	1.072	528.0	70.0	513.3	371.1	275.8	0.0342	1.45	1.42
55^o	1.072	528.0	70.0	505.7	342.7	292.9	0.0574	2.20	2.00
90^o	1.072	528.0	70.0	505.2	341.3	293.7	0.0589	2.24	2.25
90^o	0.166	600.0	70.0	[illegible]45.1	352.8	306.7	0.0596	2.37	2.25
rms error								0.11	

516 107

11. PREDICTIONS OF DHX STEADY-STATE PERFORMANCE

Figures 16 and 17 show the predicted steady-state damper position, fan speed, flows, and temperatures as a function of steady-state power. The inlet conditions for these steady-state predictions are as follows:

1) variable inlet vanes are at 75^{o},
2) remote set-point temperature is $590^{o}F$ and the module and unit offset temperature differences are $5^{o}F$,
3) inlet air temperature is $72.7^{o}F$,
4) sodium inlet temperature is $853^{o}F$ for sodium flow rates above 1.072×10^{6} lbm/hr, and
5) for sodium inlet temperatures below $853^{o}F$ the inlet sodium flow rate is 1.072×10^{6} lbm/hr.

The important features of the Figures are as follows:

1) The minimum natural convection heat transfer with the dampers closed and fan off is 0.60 MWt at an inlet sodium temperature of $591^{o}F$. Heat transfer below 0.60 MWt can only be accomplished by lowering the inlet sodium temperature. In this case, the control system cannot maintain an outlet sodium temperature of $585^{o}F$. The minimum natural convection heat transfer (0.60 MWt) is strongly dependent on how tightly the outlet dampers close. The design parameters used in the predictions of Figures 16 and 17 result in a drag coefficient of 399 velocity heads with the dampers fully closed. This corresponds to an open area of 5% of the stack flow area when the dampers are closed.
2) Maximum natural convection heat transfer is 2.74 MWt with an inlet sodium temperature of $613^{o}F$.

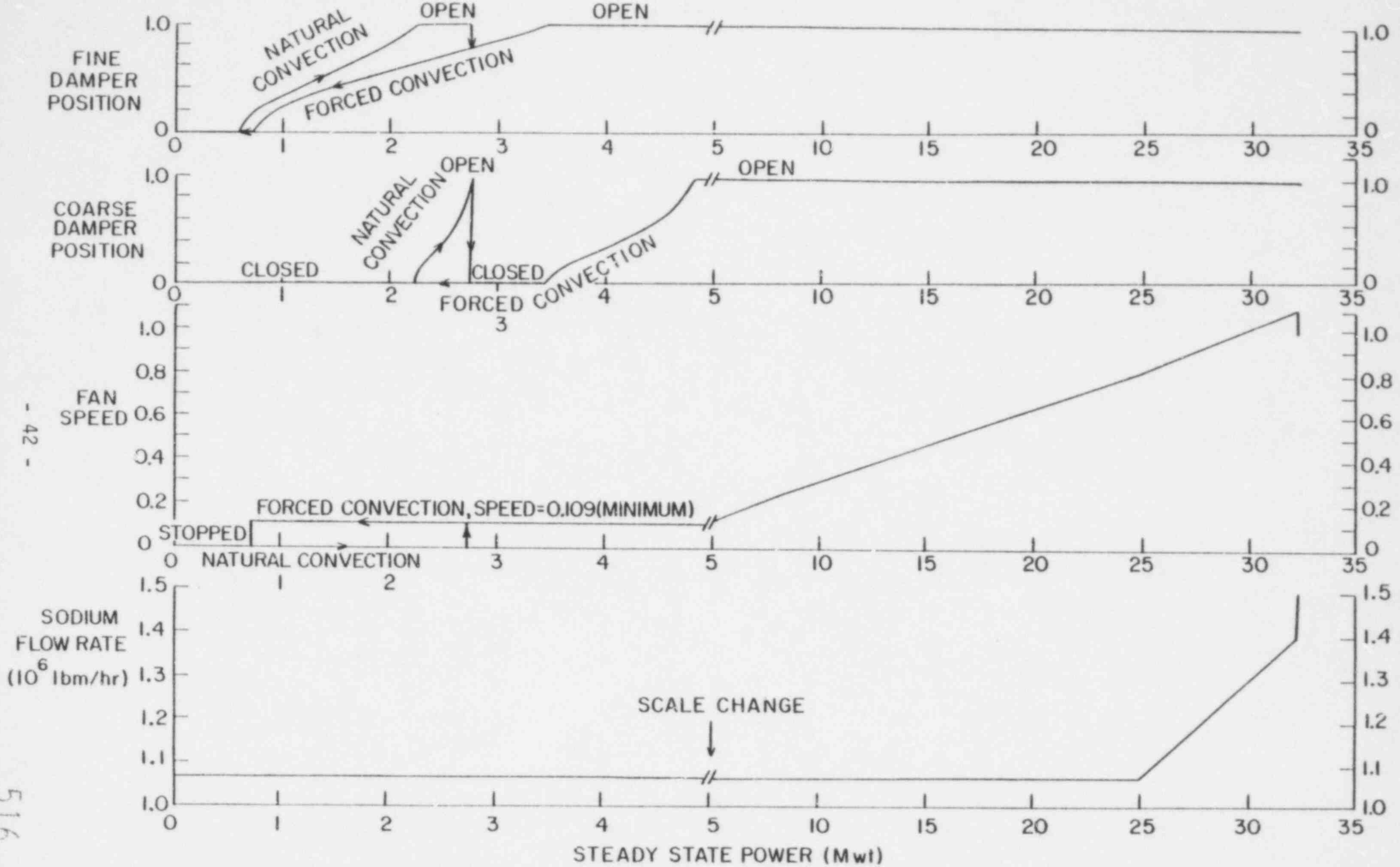

Figure 16. Damper Positions, Fan Speed, and Na Flow Rate

516 109

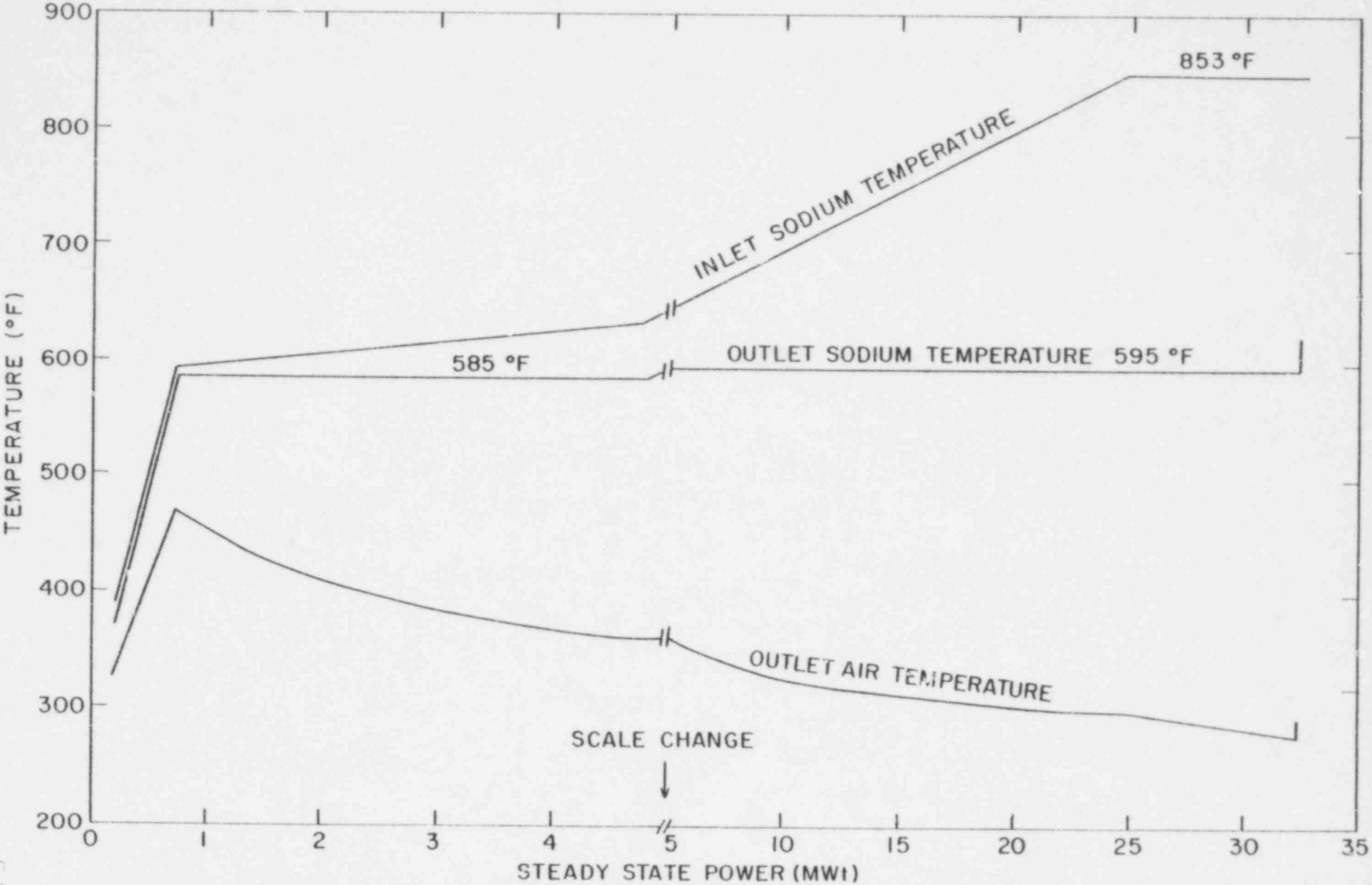

Figure 17. Sodium and Air Temperatures for Steady State

3) With the fan at minimum speed, 58 rpm, the minimum heat transfer rate is 0.75 MWt with the dampers fully closed. This number is verified by an experimental observation on the prototype FFTF/DHX reported in Reference 7, page 54. This minimum forced convection heat transfer (0.75 MWt) is strongly governed by how tightly the dampers close and verifies our choice of 5% flow area with the dampers closed.

4) Between 0.75 and 2.74 MWt the outlet sodium temperature can be held at 585^{O}F in either a natural convection mode or a forced convection mode with the fan at minimum speed. Which of these two steady-state conditions is reached depends upon the transient preceding the steady state.

5) The module control system can control the dampers up to a maximum of 4.8 MWt with the fan at minimum speed. Between 4.8 and 5.0 MWt the dampers are fully open and the fan is at minimum speed. The sodium outlet temperature rises from the module control temperature of 585^{O}F to the unit control temperature of 595^{O}F.

6) Above 5.0 MWt the unit controller maintains the outlet sodium at 595^{O}F by adjusting the fan speeds.

7) Above 32.3 MWt the fan motor and coupler are not able to drive a sufficient air flow to maintain the 595^{O}F outlet sodium temperature. This limit is demonstrated in Table 4.

In case I of Table 4 the given inlet sodium flow and temperature result is 32.31 MWt heat transfer and an outlet sodium temperature controlled to 595.0 by the unit controller (fan speed). In case II, the inlet sodium flow is increased, but now the fan is torque limited and drops in speed and flow resulting in the inability of the control system to maintain the outlet sodium temperature. This

516 111

Table 4

Comparison of Two High Power,
Forced Convection Steady-State Conditions

	Case I	Case II	Comment
Sodium flow rate, lbm/hr	1.40×10^6	1.51×10^6	given
Sodium inlet temperature, ^oF	853.0	853.0	given
Sodium outlet temperature, ^oF	595.0	614.4	Control system for Case II cannot maintain 595^oF
Fan speed, RPM	588.9	579.3	Torque limited for Case II
Air flow rate lbm/hr	2.21×10^6	2.17×10^6	
Heat transferred, MWt	32.31	32.35	

temperature rises to 614^{O}F at only a minute increase in heat transferred; i.e., from 32.31 to 32.35 MWt. Powers above about 32.4 MWt require inlet sodium temperatures above 853^{O}F. For instance, Table 2 steady state run B20, shows 36.26 MWt transferred with a sodium flow rate of 1.52 x 10^6 lbm/hr and an inlet sodium temperature of 951.4^{O}F.

516 113

12. EXAMPLES OF DHX TRANSIENTS

As a means of demonstrating the model results we have run three flow coastdown transients. Starting from a full power initial steady state determined from DHX3S we have reduced sodium flow rate from 1.14 (1.325×10^6 lbm/hr) according to the coastdown equation

$$w = \frac{1.14}{1 + t/20} \tag{38}$$

to three different low flow conditions:

A) Coastdown to $w = 0.3$

In this transient the final steady state is maintained with the dampers fully open and an adjusted fan speed.

B) Coastdown to $w = 0.1$

In this transient the final steady state is maintained with the minimum fan speed and the dampers partly closed to maintain the sodium set-point temperature.

C) Coastdown to $w = 0.03$

In this transient the final steady state is maintained with the fan breaker tripped and the dampers partly closed to maintain the sodium set-point temperature.

Table 5 shows the initial steady state and the final steady state attained for each of these three transients.

Figures 18 through 22 show sodium flow rate, sodium outlet temperature, fan speed and damper positions as a function of time for the three transients. The transients are described as follows.

TABLE 5

Initial and Final Steady States

	SODIUM			AIR				CONTROLS		
State	flow 1.163×10^6 lbm/hr	inlet temp. ^oF	outlet temp. ^oF	fan speed 532 RPM	flow 1.995×10^6 lbm/hr	inlet temp. ^oF	outlet temp. ^oF	remote setpoint temp. ^oF	fine damper position	coarse damper position
Initial	1.14	853.0	595.0	1.079 (574 rpm)	1.067	90.0	294.9	590.0	1.000	1.000
A(Final)	0.30	853.0	595.0	0.201 (107 rpm)	0.181	90.0	407.1	590.0	1.000	1.000
B(Final)	0.10	853.0	585.0	0.109 (58 rpm)	0.047	90.0	509.0	590.0	0.635	0.0
C(Final)	0.03	853.0	585.0	0.0 (0 rpm)	0.011	90.0	632.1	590.0	0.102	0.0

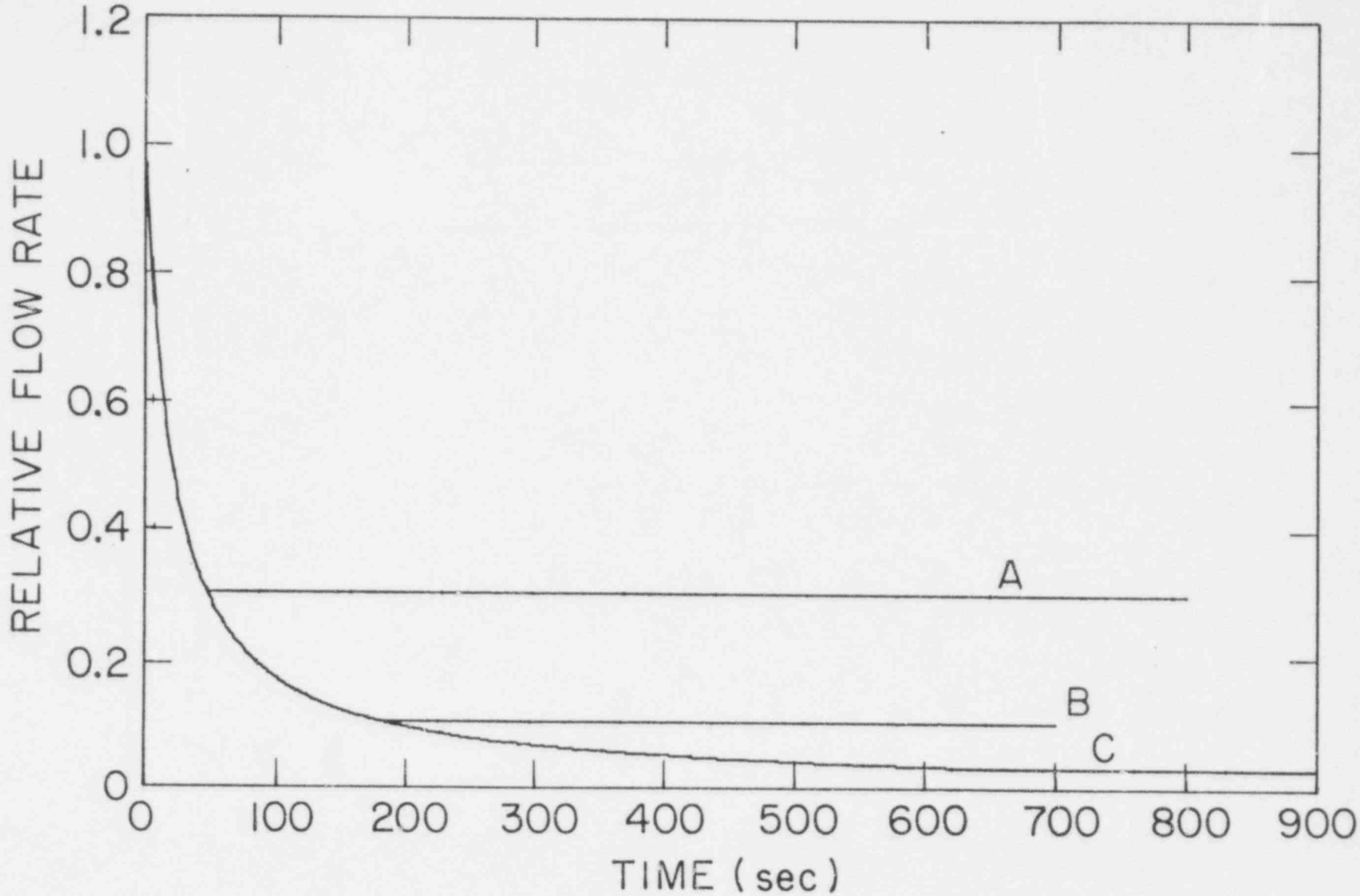

Figure 18. Sodium Flow

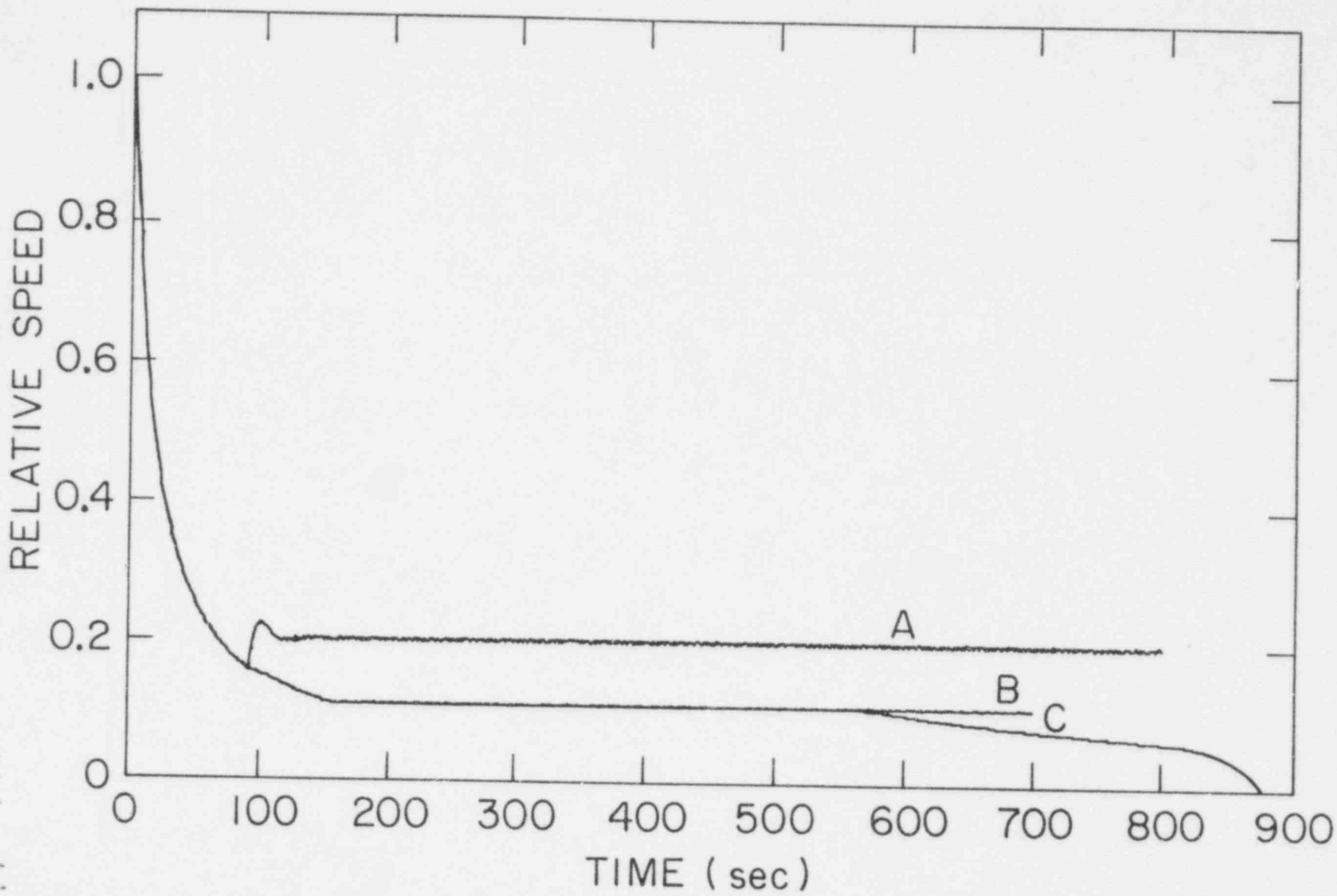

Figure 19. Fan Speed

516 117

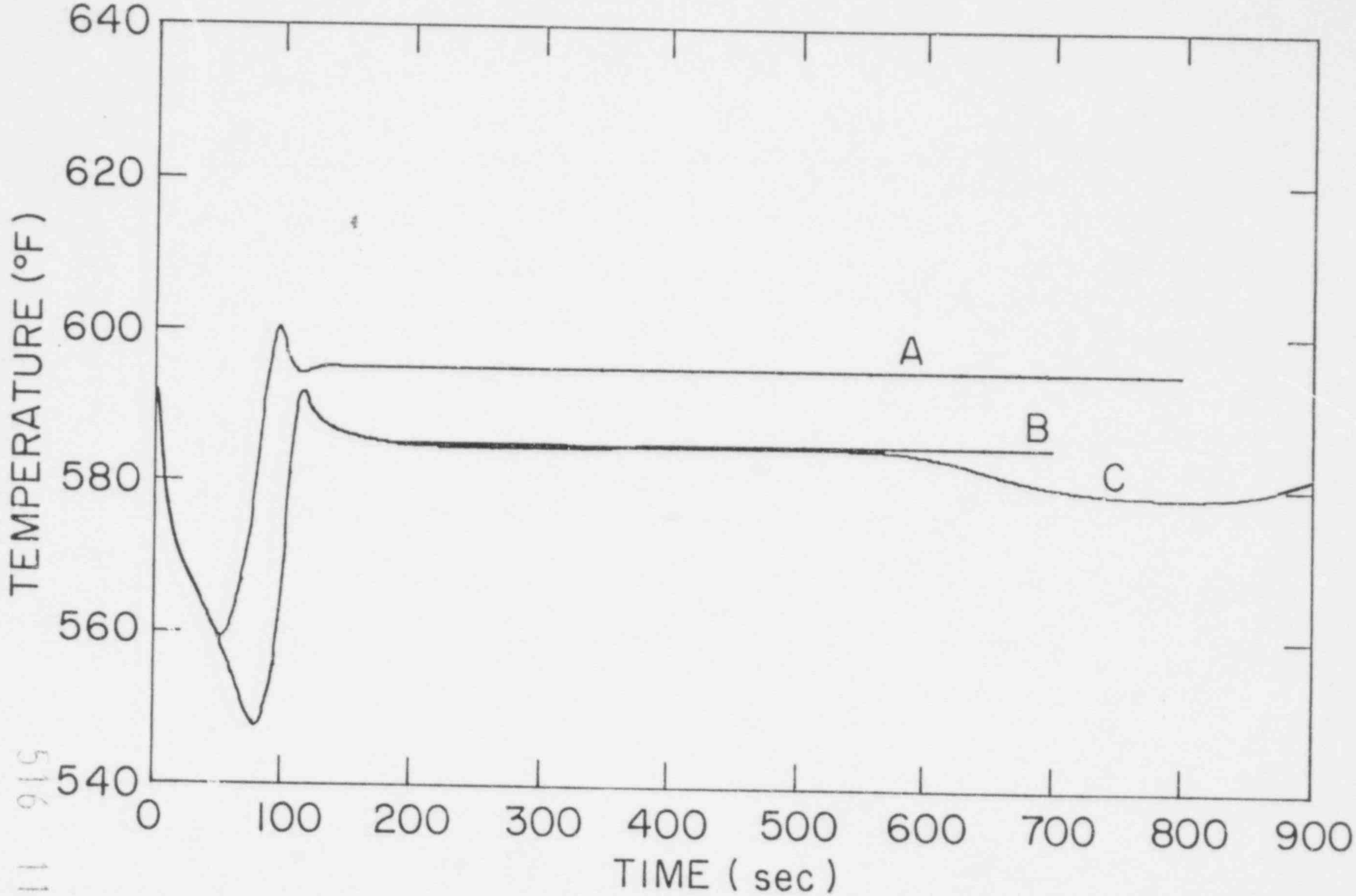

Figure 20. Sodium Outlet Temperature

516 118

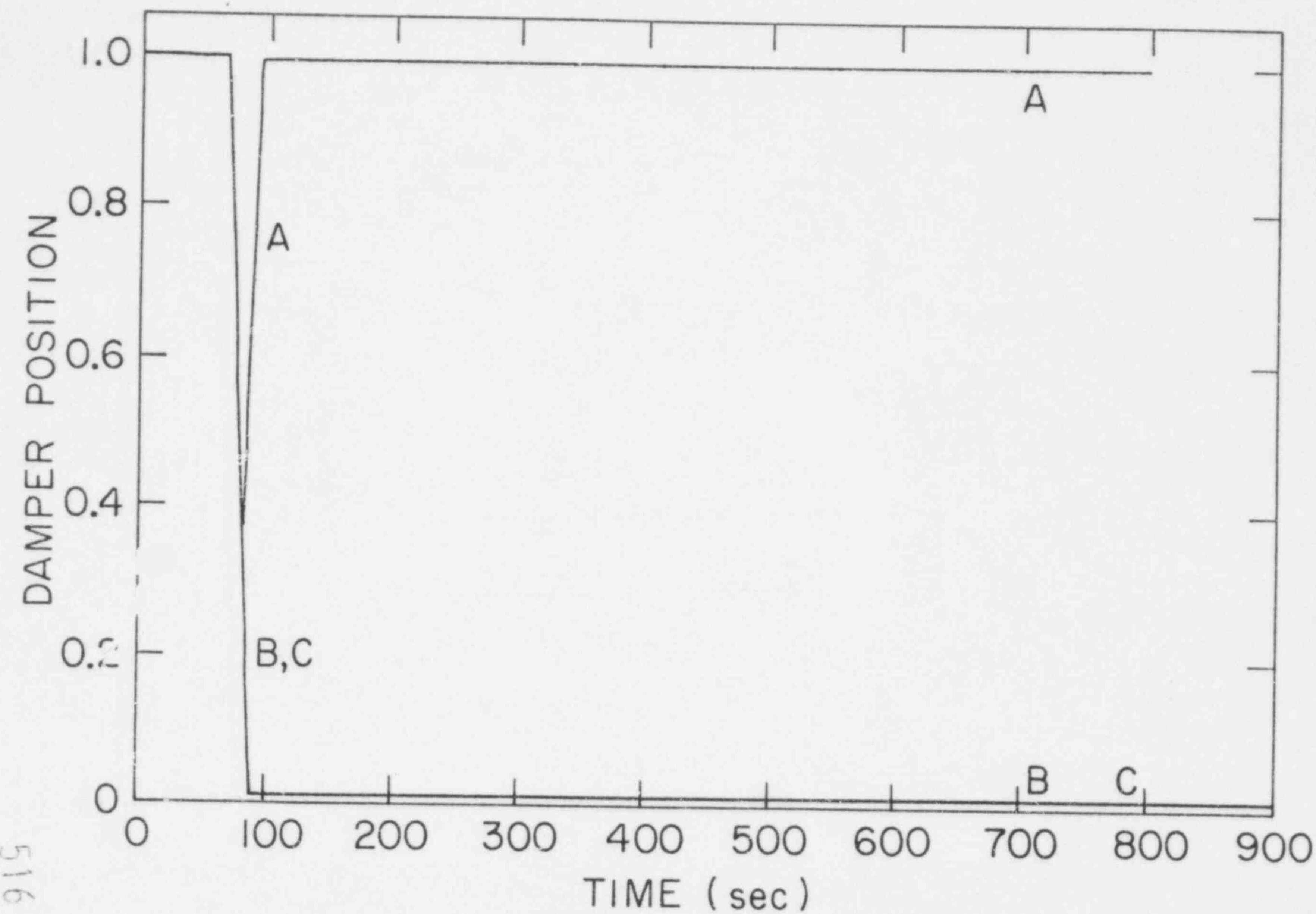

Figure 21. Coarse Damper Position

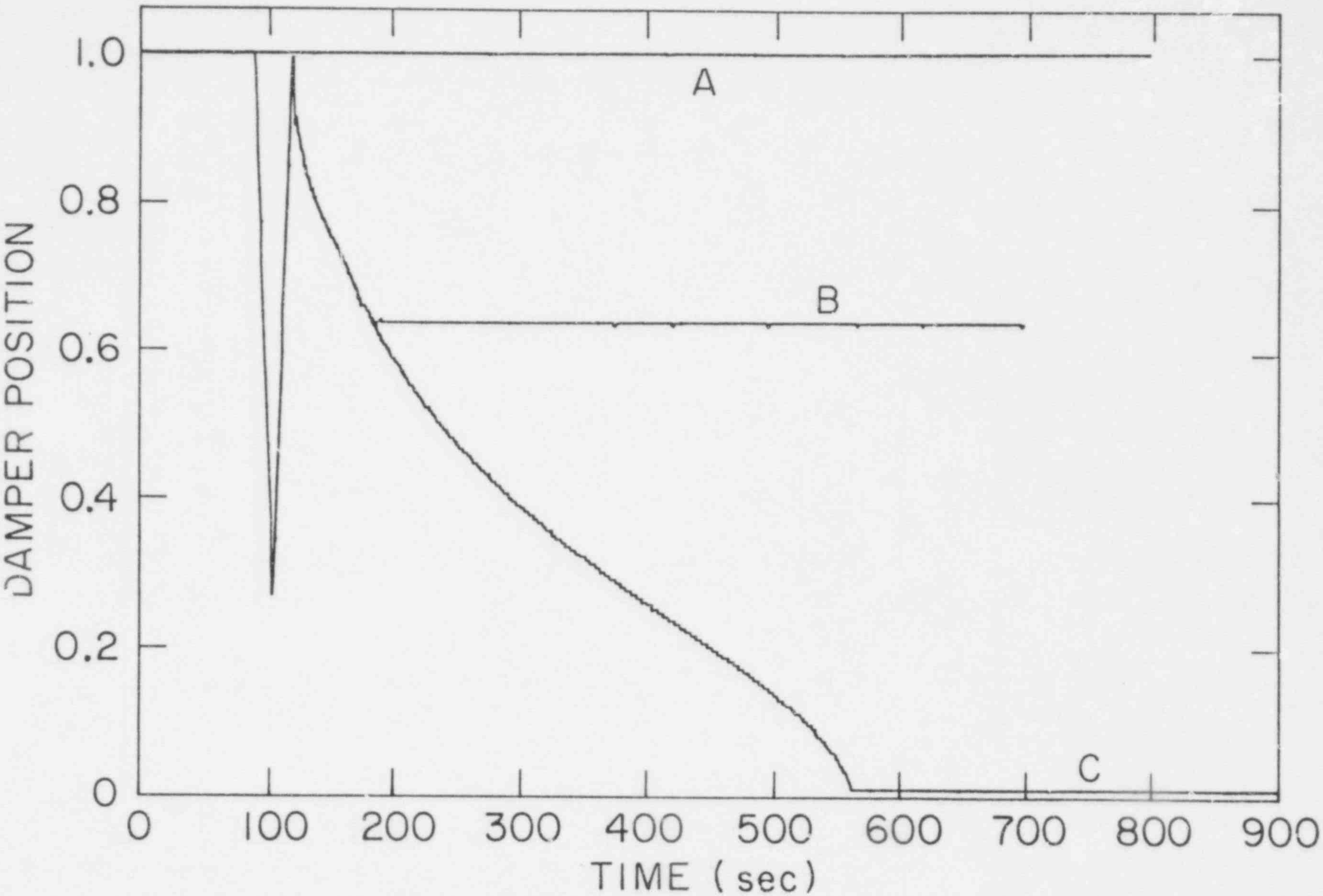

Figure 22. Fine Damper Position

516 120

A) Coastdown to 0.30 Sodium Flow

As the sodium flow coasts down the fan inertia maintains enough air flow that the outlet sodium temperature drops and the controller calls for a slower fan speed. The exciter current is reduced and the magnetic drive torque goes to zero resulting in a fan coastdown. The sodium flow has reached 0.30 at 46 seconds and the minimum sodium temperature is 559^{o}F at 50 seconds. The sodium temperature now begins to rise but because it is still below 585^{o}F the fan continues to coast down. At 67 seconds into the transient the fan speed drops below 0.2 and the damper lock-open circuit opens, releasing the dampers. The coarse damper begins to close and reaches a minimum position of 0.36 at 79 seconds. The damper reopens completely by 95 seconds and the fan speed which has reached a minimum of 0.16 at 120 seconds speeds up to 0.20. The sodium outlet temperature has returned to 595^{o}F and actually over-shoots to about 600^{o}F at 95 seconds. The transient levels off at 595^{o}F outlet sodium temperature with the dampers fully opened and the fan speed being controlled around 0.20 by the unit controller.

B) Coastdown to 0.10 Sodium Flow

The same scenerio results except that the sodium coastdown continues to a value of 0.10 at 180 seconds. The dampers unlock at the same time, 67 seconds, and the coarse damper begins to close. The minimum sodium temperature of 547^{o}F occurs at 80 seconds and the coarse damper continues to close. At 87 seconds the coarse dampers are fully closed and the fine dampers begin to close because the sodium temperature, although rising, is way below 585^{o}F. The minimum fine damper position is 0.27 at 102 seconds and then reopens momentarily at 118 seconds before closing to 0.635 at the final steady state. The maximum sodium temperature is 592^{o}F at 115 seconds and the final fan speed is 0.109, the minimum demanded speed. The final sodium temperature of 585^{o}F is maintained by the fine dampers controlled by the module controller.

C) Coastdown to 0.03 Sodium Flow

The transient begins the same as the previous two transients, however, the sodium flow coastdown continues to 0.03 at 650 seconds. The fan coasts down to a minimum speed and is held there from 160 seconds to 565 seconds. By this time both coarse and fine dampers are fully closed and the continuing sodium flow coastdown caused the outlet sodium temperature to fall below 585^{o}F. This trips the fan breaker and the fan coasts down slowly to 0.065 where low speed friction takes over and causes it to stop at 880 seconds. The sodium temperature slowly rises to 585^{o}F and will eventually be held at 585^{o}F by the fine damper opening to 0.10. This is a natural circulation condition.

516 122

APPENDIX A

Summary of Code Variables, Parameters, and Equations

The DHX Code has two versions, a transient version and a steady-state version. Table A1 lists the thirty-one process variables calculated by the seven subroutines. Figure 1 of the Introduction (Chapter 1) shows the relationship of these variables to each other.

Any run, steady state or transient, requires six reference state variables to be input by the user. We recommend the following reference values based, in part, on experimental observations on the prototype FFTF HTS/DHX;[7] June 21, 1975, 14:39 to 14:43:

Reference State Variables

T_{3r}, inlet sodium temperature, ^oF	771.3
T_{or}, inlet air temperature, ^oF	72.7
T_{1r}, outlet air temperature, ^oF	259.7
T_{2r}, outlet sodium temperature, ^oF	521.7
S_r, motor slip,	0.02
θ_r, variable-inlet-vane angle, ^{o}	78.9
Normalizations	
fan speed, RPM	532.0
sodium flow rate, 10^6 lbm/hr	1.163
air flow rate, 10^6 lbm/hr	1.995

The remaining twenty-five reference state variables are defined by the code or are calculated by the code.

Table A1

Process Variables

	Reference state[a]	Steady state[a]
Subroutine REST3T:		
w, relative sodium flow	1.0	specify
T_3, inlet sodium temperature, ^oF	specify	specify
T_s, remote set-point temperature, ^oF		specify
T_o, air inlet temperature, ^oF	specify	specify
K_s, scram index, 0/1 = normal/scram	0	0
Subroutine HX3T:		
T_1, outlet air temperature, ^oF	specify	
T_2, outlet sodium temperature, ^oF	specify	
$\Delta T_{\ell m}$, log-mean-temperature difference, ^oF		
Subroutine BUOY3T:		
ΔP, buoyant head, inches of H_2O		
T, mean stack temperature, ^oF		
Subroutine CNTR3T:		
T_m, measured sodium temperature, ^oF		
I_u, unit controller integral, ^oF-sec		
I_m, module controller integral, ^oF-sec		
α_D, demanded speed	1.0	
X, damper signal	1.0	
K, fan breaker index, 0/1 - open/closed	1	specify

516 124

Table A1 (Cont.)

Subroutine DRIV3T:	Reference state[a]	Steady state[a]
S, motor slip	specify	
α_M, motor speed	1.0	
β_M, motor torque	1.0	
ΔS, magnetic drive slip		
I, relative motor current		
β_c, magnetic drive torque	1.0	
Subroutine FAN3T:		
α, relative speed	1.0	
ν, relative flow	1.0	
δ, relative head	1.0	
β, relative torque	1.0	
θ, variable inlet vane angle, ^{o}	specify	specify
Subroutine DAMP3T:		
L, lock open index 0/1 = released/locked open	1	
X_f, fine damper position, 0→1 = closed→open	1.0	
X_c, coarse damper position, 0→1 = closed→open	1.0	
K_d, drag coefficient of dampers.		

[a] "Specify" means the user must input a value for these variables. A number such as 1.0, 1, 0 means the code furnishes these automatically. A blank entry means that the number is calculated by the code.

516 125

A steady state run also requires six variables to be specified:

w, relative sodium flow rate,

T_3, inlet sodium temperature, ^oF

T, remote set-point temperature, ^oF,

T_0, air inlet temperature, ^oF,

K, fan breaker index, 0/1 = open/closed, and

θ, variable inlet vane angle, ^{o}.

The other twenty-five variables are determined by the steady-state version of the code. A steady-state run is a fictitious transient, where many of the time constants are shortened to zero. We recommend a time of about 10 seconds with a timestep of 0.2 seconds.

For a transient run, in addition to the reference state inputs, initial conditions for all thirty-one reference variables are required. These initial conditions are normally the result of a previous steady-state run, or a restart of a transient run. During a transient run, the five REST3T variables are either to be specified functions of time or REST3T is to be replaced by other SSC subroutines. We have experimented with timesteps and recommend 0.2 seconds as being suitable for DHX3T. Larger timesteps lead to inaccuracies and timesteps shorter than 0.1 seconds are not necessary.

The following pages of this appendix list the variables, parameters, and equations used in DHX3T and DHX3S.

Subroutine REST3T and REST3S

Defined Variables

The five variables driving a DHX transient are:

w, relative sodium flow rate,

T_3, inlet sodium temperature, ^oF,

T_s, remote set-point temperature, ^oF,

T_o, air inlet temperature, ^oF, and

K_s, scram index, 0/1=normal/scrammed.

Required Variables

The following reference value is required:

T_{2r}, reference outlet sodium temperature, ^oF.

Input Parameters

The unit controller uses $\Delta T = 5.0$, the set-point offset temperature difference, ^oF.

Calculated Reference State Parameters and Variables

The five reference state variables are:

$w_r = 1.0$, reference sodium mass flow rate,

T_{3r} = (specify), reference inlet sodium temperature, ^oF,

T_{or} = (specify), reference inlet air temperature, ^oF,

$K_{sr} = 0$, reference scram index, and

$T_{sr} = T_{2r} - \Delta T$, reference set-point temperature.

Transient Equations (REST3T)

Each of the five defined variables are specified functions of time.

Steady-State Equations

Each of the five defined variables are to be specified constants.

Subroutine HX3T and HX3S

Defined Variables

Three process variables are calculated:

T_2, outlet sodium temperature, ^oF,

T_1, outlet air temperature, ^oF, and

$\Delta T_{\ell m}$, log mean temperature difference, ^oF.

Required Variables

Four process variables and four reference state variables are used by this subroutine:

T_o, inlet air temperature, ^oF,

T_3, inlet sodium temperature, ^oF,

ν, relative air mass flow rate,

w, relative sodium mass flow rate,

T_{or}, reference inlet air temperature, ^oF,

T_{1r}, reference outlet air temperature, ^oF,

T_{2r}, reference outlet sodium temperature, ^oF, and

T_{3r}, reference inlet sodium temperature, ^oF.

Input Parameters

Only one input parameter specifies the heat exchanger, the rest are physical constants:

τ_r = 12.07, reference state value of sodium time constant, sec,

$$A_i = \begin{Bmatrix} 59.57 \\ -7.950\ E\text{-}3 \\ -2.872\ E\text{-}7 \\ 6.035\ E\text{-}1 \end{Bmatrix}$$, coefficients of sodium density,(7)

$$B_i = \begin{Bmatrix} 0.3457 \\ -7.923\ E\text{-}5 \\ 3.409\ E\text{-}9 \end{Bmatrix}$$, coefficients of sodium heat capacity,(7) and

516 128

T_a = 459.7, absolute temperature at 0 ^oF, ^oR.

Calculated Reference State Parameters

The reference state determines the heat transfer ratios ξ_{1r} and ξ_{2r}:

$T_r = (T_{3r} + T_{2r})/2$, sodium temperature, ^oF,

$C_{pr} = B_1 + B_2T_r + B_3T_r^2$, sodium heat capacity, Btu/lbm - ^oF,

$\rho_r = A_1 + A_2T_r + A_3T_r^2 + A_4T_r^3$, sodium density, lbm/ft^3,

$$\Delta T_{\ell mr} = \frac{(T_{3r} - T_{1r}) - (T_{2r} - T_{or})}{\ell n \left(\frac{T_{3r} - T_{1r}}{T_{2r} - T_{or}}\right)}$$, reference log mean temperature difference, ^oF,

$\xi_{1r} = (T_{1r} - T_{or})/\Delta T_{\ell mr}$, reference air heat transfer ratio, and

$\xi_{2r} = (T_{3r} - T_{2r})/\Delta T_{\ell mr}$, reference sodium heat transfer ratio.

Transient Equations (HX3T)

The transient code computes in the following order:

$T = (T_3 + T_2)/2$, mean sodium temperature, ^oF,

$\rho = A_1 + A_2T + A_3T^2 + A_4T^3$, sodium density, lbm/ft^3 ,

$C_p = B_1 + B_2T + B_3T^2$, sodium heat capacity, Btu/lbm - ^oF ,

$$\tau = \frac{\tau_r \rho}{w \rho_r}$$, sodium time constant, sec ,

$$T_r = \frac{T_o + T_1 + 2T_a}{T_{or} + T_{1r} + 2T_a}$$, temperature ratio ,

$\xi_1 = \xi_{1r} T_r^{0.21} \nu^{-0.30}$, air heat transfer ratio,

$$\xi_2 = \frac{\xi_{2r} C_{pr}}{w C_p} T_r^{0.21} \nu^{0.70}$$, sodium heat transfer ratio ,

$$\Delta T_{\ell m} = \frac{(T_3 - T_1) - (T_2 - T_o)}{\ell n \frac{T_3 - T_1}{T_2 - T_o}}$$, log mean temperature difference, ^oF ,

516 129

$$\frac{dT_2}{dt} = (T_3 - T_2 - \xi_2 \, \Delta T_{\ell m})/\tau,$$ time derivative of sodium temperature, $^oF/sec$,

$$\theta_2 = \frac{T_2 - T_o}{T_3 - T_o}$$, dimensionless outlet sodium temperature ,

$$\theta = \left[\theta - \frac{\theta - \xi_1\left(\frac{1 - \theta - \theta_2}{\ell n(\frac{1-\theta}{\theta_2})}\right)}{1 + \frac{\xi_1}{\ell n\left(\frac{1-\theta}{\theta_2}\right)}\left(1 - \frac{1 - \theta - \theta_2}{(1 - \theta)\ \ell n\ (\frac{1-\theta}{\theta_2})}\right)} \right]$$ iteratively 10 times, and

$$T_1 = T_o + \theta\ (T_3 - T_o)$$, outlet air temperature ^oF

Steady-State Equations (HX3S)

The steady-state version of the subroutine is similar to the transient version except both T_1 and T_2 are determined from a Newton-Raphson iteration scheme:

$$\theta_2 = \frac{T_2 - T_o}{T_3 - T_o}$$, dimensionless sodium temperature,

$$\theta_1 = \xi_1 \left(\frac{1 - \theta_1 - \theta_2}{\ell n\left(\frac{1 - \theta_1}{\theta_2}\right)}\right)$$, iteratively by Newton-Raphson,

$$T_1 = T_o + \theta_1\ (T_3 - T_o)$$, air outlet temperature, ^oF,

$$\theta_2 = 1 - \xi_2 \left(\frac{\theta_1 - (1 - \theta_2)}{\ell n\left(\frac{\theta_2}{1 - \theta_1}\right)}\right)$$, iteratively by Newton-Raphson, and

$$T_2 = T_o + \theta_2\ (T_3 - T_o)$$, sodium outlet temperature.

Subroutine BUOY3T and BUOY3S

Defined Variables

The process variables computed are:

T, stack temperature, ^oF, and

ΔP, buoyant head, in inches of H_2O.

Required Variables

The following are required from other subroutines:

ν, relative air flow rate,

T_o, inlet air temperature, ^oF,

T_1, outlet air temperature, ^oF,

T_{or}, reference inlet air temperature, ^oF, and

T_{1r}, reference outlet air temperature, ^oF.

Input Parameters

The stack is characterized by two parameters and three physical constants:

τ_o = 0.857 , reference value of time constant, sec,

H = 30.0 , effective stack height, ft,

R = 0.3702 , gas constant, psi-ft^3/lbm-^oR,

P_o = 406.8 , atmospheric pressure, in inches of H_2O, and

T_a = 459.7 , absolute temperature at 0 ^oF, ^oR.

Calculated Reference State Parameters and Variables

The following calculates the reference values:

$$\Delta P_r = \frac{P_o H}{144R}\left(\frac{1}{T_{or} + T_a} - \frac{1}{T_r + T_a}\right)$$ buoyant head, in inches of H_2O, and

516 131

$T_r = T_{1r}$, stack temperature, ^{o}F.

Transient Equations BUOY3T

The transient version utilizes the equations:

$$\tau = \frac{T + T_a}{T_o + T_a} \tau_o$$, stack time constant, sec,

$$\frac{dT}{dt} = \frac{\nu}{\tau} (T_1 - T)$$, time derivative of stack temperature, ^{o}F/sec, and

$$\Delta P = \frac{P_o H}{144R} \left(\frac{1}{T_o + T_a} - \frac{1}{T + T_a} \right)$$, buoyant head, in inches of H_2O.

Steady-State Equations BUOY3S

$T = T_1$, stack temperature, ^{o}F, and

$$\Delta P = \frac{P_o H}{144R} \left(\frac{1}{T_o + T_a} - \frac{1}{T + T_a} \right)$$, buoyant head, in inches of H_2O.

516 132

Subroutine CNTR3T and CNTR3S

Defined Variables

The six variables are:

T_m, measured sodium temperature, ^oF,

I_u, unit controller integral, ^oF-sec,

I_M, module controller integral, ^oF-sec,

α_D, demanded speed,

χ, damper position signal, and

K, fan breaker index, 0/1 - open/closed.

Required Variables

Five variables are needed from other subroutines:

T_2, outlet sodium temperature, ^oF,

T_s, remote set-point temperature, ^oF,

T_{2r}, reference outlet sodium temperature, ^oF,

χ_f, fine damper position (0. = closed, 1. = open), and

χ_c, coarse damper position (0. = closed, 1. = open).

Input Parameters

The control system parameters are:

α_{max} = 1.12 , maximum demanded fan speed,

α_{min} = 0.109 , minimum demanded fan speed,

ΔT_u = 5.0 , unit controller temperature offset, ^oF,

ΔT_M = 5.0 , module controller temperature offset, ^oF,

τ_m = 1.0 , sodium temperature measurement delay, sec,

g_u = 0.01 , unit controller gain, $^oF^{-1}$,

r_u = 0.2 , unit controller repetition rate, sec^{-1},

$S_u = 1.0$, unit controller derivative time, sec,

$g_M = 0.1$, module controller gain, $^oF^{-1}$,

$r_M = 0.02$, module controller repetition rate, sec^{-1},

$S_M = 5.0$, module controller derivative time, sec, and

$\Delta X = 0.015$, damper position to trip fan breaker.

Calculated Reference State Parameters and Variables

The reference values of the six variables are given as:

$T_{mr} = T_{2r}$, reference measured sodium temperature, ^oF,

$I_{ur} = \frac{1}{g_u r_u}$, reference unit controller integral, ^oF-sec,

$I_{Mr} = \left[(\frac{1}{g_M} - \Delta T_u - \Delta T_M)/r_M\right] \geq 0$, reference module controller integral, ^oF-sec,

$\alpha_{Dr} = 1.0$ reference demanded speed,

$x_r = 1.0$ reference damper signal (open), and

$K_r = 1$ reference fan breaker index (closed).

Transient Equations CNTR3T

The transient equations are:

$\frac{dT_m}{dt} = (T_2 - T_m)/\tau_m$, time derivative of measured sodium temperature, ^oF/sec,

$E_u = T_m - T_s - \Delta T_u$, unit controller temperature error, ^oF,

$\frac{dI_u}{dt} = E_u$, time derivative of unit controller integral, ^oF,

516 134

$$\alpha_D = g_u \left[E_u + r_u I_u + \frac{\tau_u}{\tau_m}(T_2 - T_m)\right] \text{, demanded speed,}$$

$$\text{if} \begin{Bmatrix} \alpha_D \leq \alpha_{min} \; ; \; \alpha_D = \alpha_{min} \\ \alpha_D \geq \alpha_{max} \; ; \; \alpha_D = \alpha_{max} \end{Bmatrix} \text{, limits demanded speed,}$$

$E_M = T_m - T_s + \Delta T_M$, module controller temperature error, ^oF,

$\frac{dI_M}{dt} = E_M$, time derivative of module controller integral, ^oF,

$$\chi = g_M \left[E_M + r_M I_M + \frac{\tau_M}{\tau_m}(T_2 - T_m)\right] \text{, damper signal,}$$

$$\text{if} \begin{Bmatrix} \chi \leq 0, \; \chi = 0 \\ \chi \geq 1, \; \chi = 1 \end{Bmatrix} \text{, limits damper signal,}$$

if $\chi \leq 0$ and $X_f \leq \Delta X$ and $X_c \leq \Delta X$, $K = 0$, opens fan breaker if dampers are closed and module controller is calling for less flow, and

if $X \geq 1$ and $X_c \geq 1 - \Delta X$, $K = 1$, closes fan breaker if dampers are open and module controller is calling for more flow.

The unit controller integral, I_u, has roll-down and roll-up limits of

$$\frac{\alpha_{min}}{r_u g_u} < I_u < \frac{\alpha_{max}}{r_u g_u} \text{ ,}$$

and the module controller integral has limits of

$$0 < I_M < \frac{-1}{r_M g_M} \text{ .}$$

<u>Steady-State Equations CNTR3S</u>

$T_m = T_2$, measured sodium temperature, ^oF

516 135

$E_u = T_m - T_s + \Delta T_u$, unit controller temperature error, ^oF,

if $|E_u| \geq 10$, $E_u = 10$ sign (E_u), limits error to 10^oF,

$\frac{dx_D}{dt} = 0.001\ E_u$, drives demanded speed signal proportional to temperature error, sec^{-1},

$$\text{if} \begin{Bmatrix} \alpha_D \leq \alpha_{min}, \ \alpha_D = \alpha_{min} \\ \alpha_D \geq \alpha_{max}, \ \alpha_D = \alpha_{max} \end{Bmatrix}$$ limits demanded speed,

$E_M = T_m - T_s + \Delta T_M$, module controller temperature error, ^oF,

if $|E_M| \geq 10$, $E_M = 10$ sign (E_u), limits error to 10^oF,

$\frac{dx}{dt} = 0.001\ E_M$, drives damper control signal proportional to temperature error, sec^{-1}, and

$$\text{if} \begin{Bmatrix} x \leq 0, \ x = 0 \\ x \geq 1, \ x = 1 \end{Bmatrix}$$, which limits the damper signal.

Subroutine DRIV3T and DRIV3S

Defined Variables

Six variables are defined:

S, motor slip,

α_M, relative motor speed,

β_M, relative motor torque,

ΔS, magnetic drive slip,

I, relative motor current, and

β_C, magnetic drive torque,

Required Variables

These are the following:

α_D, demanded speed,

α, relative fan speed,

K, fan breaker index, and

S_r, reference motor slip (specified).

Input Parameters

The motor and magnetic drive design parameters are given by:

S_o = 0.208 , motor slip at maximum torque,

a = 0.666 , motor torque parameter,

τ_M = 1.446 , motor inertia time constant, sec,

Q_M = 18,600., maximum magnetic drive torque, ft-lbf,

N_s = 600. , synchronous speed, RPM,

N_r = 532. , reference fan speed, RPM,

516 137

$$C_i = \begin{Bmatrix} 0.5 \\ 0.014 \\ 0.036 \\ 0.4 \\ 0. \end{Bmatrix}$$, five magnetic drive torque coefficients,

$\tau = 0.0001$, time to drive exciter to full current per unit speed error, sec, and

$Q_r = 12{,}122.$, reference magnetic drive torque, ft-lbf.

Calculated Reference State Parameters and Variables

Reference state values are given by:

$$K_r = \frac{S_r^{\ 2} + aS_r + S_o^{\ 2}}{(2S_o + a)\ S_r}$$, reference motor torque constant,

$\alpha_{Mr} = 1.0$, reference motor speed,

$\beta_{Mr} = 1.0$, reference motor torque,

$\beta_{cr} = 1.0$, reference magnetic drive torque, and

$\Delta S_r = 1 - S_r - \frac{N_r}{N_s}$, reference magnetic drive slip.

The following secant iteration scheme gives the reference magnetic drive current required to generate the reference magnetic drive torque:

$$I_1 = 1.0 \ ,$$

$$I_2 = \frac{I_1}{\beta_1} \ ,$$

$$I_{i+1} = I_i - (\beta_i - 1.0)\left(\frac{I_i - I_{i-1}}{\beta_i - \beta_{i-1}}\right) , \ i = 2,3, \ . \ . \ . \ 10,$$

where $\beta(I)$, the torque for a given current is determined as follows:

$$K_c = \frac{Q_m}{Q_r}\left[C_1 \ I + (1 - C_1) \ I^2\right] ,$$

516 138

$\sigma = C_2 + C_3 I$, slip at maximum torque,

$\gamma = C_4 + C_5 I$, torque at full slip,

$$A = \frac{\gamma (1 + \sigma^2) - 2\sigma}{1 - \gamma} \text{ , and}$$

$$\beta(I) = \frac{K_c \Delta S_r (2\sigma + A)}{(\Delta S_r)^2 + A \Delta S_r + \sigma^2} \text{ , relative torque.}$$

Transient Equations DRIV3T

An iteration scheme uses I (current) and α (fan speed) and adjusts the motor speed and magnetic drive slip such that the torques of the motor and magnetic drive are equal. The slips are related by:

$$\Delta S = 1 - S - \alpha \frac{N_r}{N_s} .$$

We choose an initial pair $(S, \Delta S)$ by setting

$$\Delta S_1 = 0$$

and a second pair $(S, \Delta S)$ by setting

$$S_2 = 0.$$

We have the magnetic drive torque for the n-th iteration as

$$\beta_{c,n} = \frac{K_c \Delta S_n (2\sigma + A)}{(\Delta S_n)^2 + A\Delta S_n + \sigma^2} ,$$

where K_c, σ, γ, and A are functions of I given above. The motor torque is given by:

$$\beta_{M,n} = \frac{K_r (2S_o + a) S_n}{S_n^2 + aS_n + S_o^2} .$$

516 139

We then iterate 12 times for the motor slip:

$$S_{n+1} = \frac{S_n - \left(\dfrac{\beta_{C,n} - \beta_{M,n}}{\beta_{C,n-1} - \beta_{M,n-1}}\right) S_{n-1}}{1 - \left(\dfrac{\beta_{C,n} - \beta_{M,n}}{\beta_{C,n-1} - \beta_{M,n-1}}\right)} , \quad n = 2, 3, \ldots 12 .$$

At convergence the β's are equal and we have S, ΔS, β_C, and β_M, for a given current and fan speed.

The exciter current is determined from

$$\frac{dI}{dt} = (\alpha_D - \alpha)/\tau$$, and is limited between 0 and 1.

The time constant τ is taken to be very small and the exciter current is usually 0 or 1 [illegible]l current) except for very small speed errors.

Steady-State DRIV3T

The steady-state version is identical to the transient version.

Subroutine FAN3T and FAN3S

Defined Variables

The fan subroutine determines the air flow characteristics of the fan and the variable inlet vanes:

α, relative fan speed,

ν, relative fan flow,

δ, relative fan head

β, relative fan torque, and

θ, variable inlet vane angle, ^{o}.

Required Variables

The required variables are:

β_c, magnetic drive torque,

ΔP, buoyant head, in inches of H_2o,

ΔP_r, reference buoyant head, in inches of H_2O,

T_o, inlet air temperature,

T_1, outlet air temperature,

K_d, drag coefficient of dampers,

K_s, scram index,

α_D, demanded speed, and

K, fan breaker index.

Input Parameters

The design parameters are:

τ = 16.0 , fan inertia time constant, sec,

A = 0.04 , a fan friction coefficient

α_o = 0.065 , a fan speed below which friction is effective,

$F = 20.$, variable inlet vane drive speed, ^{o}/sec,

$\theta_{max} = 75.$, maximum vane angle, ^{o},

$\theta_{min} = 0.$, minimum vane angle,

$N = 10.$, number of iterations,

$$e_i = \begin{Bmatrix} 60.0 \\ 0.001 \\ 0. \end{Bmatrix}$$, variable inlet vane coefficients,

$$a_i = \begin{Bmatrix} 1.17 \\ 0.24 \\ 0. \\ -0.10 \\ -0.31 \end{Bmatrix}$$, fan head coefficients for $\nu \leq \alpha$,

$$b_i = \begin{Bmatrix} 3.4 \\ 3.0 \\ 3.9 \\ -2.5 \\ 0. \end{Bmatrix}$$, fan head coefficients for $\nu > \alpha$,

$$C_i = \begin{Bmatrix} 0.31 \\ 0.85 \\ 0. \\ -0.04 \\ -0.12 \end{Bmatrix}$$, fan torque coefficients for $\nu \leq \alpha$,

$$d_i = \begin{Bmatrix} -1.0 \\ 2.6 \\ -0.95 \\ 0.35 \\ 0. \end{Bmatrix}$$, fan torque coefficients for $\nu > \alpha$,

$H = 7.0$, reference fan head, in inches of H_2O,

$G = 15{,}000$, reference mass velocity of air, lbm/hr - ft^2,

$\eta_o = 0.80$, reference fan efficiency,

$P_o = 406.8$, atmospheric pressure, in inches of H_2O,

$\gamma = 1.3990$, ratio of specific heats for air,

$$C = 2.436 \times 10^6 = \left(\frac{14.696 \times 12 \times 3600}{406.8}\right)^2$$, a physical constant, $\left(\frac{\text{psi-sec}}{\text{ft } H_2O\text{-hr}}\right)^2$,

$g_o = 32.174$, a dimensional constant lbm-ft/lbf-sec^2 ,

$R = 0.3702$, gas constant, psi-ft^3/lbm-^{o}R, and

$T_a = 459.7$, absolute temperature at 0^{o}F, ^{o}R.

516 142

Calculated Reference State Parameters and Variables

The reference state parameters are calculated as follows:

$P_a = P_o + H$, reference fan discharge pressure, in inches of H_2O,

$$T = (T_{or} + T_a)\left[1 + \frac{\left(\frac{P_a}{P_o}\right)^{\frac{\gamma-1}{\gamma}} - 1}{\eta_o}\right]$$, reference fan discharge absolute temperature, ^oR,

$$r = \frac{P_a}{P_o - \Delta P_r}$$, reference pressure ratio across heated tubes,

$$t = \frac{T_{1r} + T_a}{T}$$, reference temperature ratio across heated tubes,

$$K_o = 2\left[\left(\frac{Cg_o}{RG^2}\right)\frac{P_a^2}{T}\frac{(1 - \frac{1}{r^2t})}{(1 + \frac{\ell n(rt)}{\ell n(r)})} - \ell n(rt)\right]$$, reference drag coefficient across heated tubes.

The reference state variables are the following:

$\alpha_r = 1.0$, reference fan speed,

$\nu_r = 1.0$, reference air flow rate,

$\delta_r = 1.0$, reference fan head,

$\beta_r = 1.0$, reference fan torque, and

$\theta_r =$ (specify) , reference variable inlet vane angle, ^{o}.

Transient Equations (FAN3T)

Differential equations describe the variable inlet-vane angle and the fan speed. These equations are:

$$\frac{d\theta}{dt} = - K_s F ,$$

$$\theta = \begin{cases} \theta_{min}, \text{ if } \theta \leq \theta_{min} \\ \theta_{max}, \text{ if } \theta \geq \theta_{max} \end{cases}$$, which limits θ

$$\beta_f = \begin{cases} \beta_c, \text{ if } \alpha \leq 0 \\ A\,(1 - \frac{\alpha}{\alpha_o}), \text{ if } \alpha \leq \alpha_o \\ 0, \text{ if } \alpha > \alpha_o \end{cases}$$, frictional torque, and

516 143

$\frac{d\alpha}{dt} = (\beta_c - \beta - \beta_f)/\tau$, the time rate of change of fan speed.

The fan characteristics and resistance of the variable inlet vanes, the heated finned tubes, and the dampers give the following equations solved iteratively:

$$h = \left[e_1 \left(e_2^{\theta/75} - e_2\right) + e_3 \left(1 - \frac{\theta}{75}\right)\right]\nu^2$$, resistance head of variable inlet vanes, $0 \leq 75^\circ$,

$$\delta = -h + \begin{cases} \alpha^2 \sum_{i=1}^{5} a_i \left(\frac{\nu}{\alpha}\right)^{i-1}, & \text{if } \nu \leq \alpha \\ \nu^2 \sum_{i=1}^{5} b_i \left(\frac{\alpha}{\nu}\right)^{i-1}, & \text{if } \alpha < \nu \end{cases}$$, f n head minus variable inlet vane resistance head,

$$\eta = \frac{\delta\nu}{\beta\alpha}$$, fan efficiency,

$$P_a = P_o + H\,\delta$$, fan discharge pressure, in inches of H_2O,

$$r = \frac{P_a}{P_o - \Delta P}$$, pressure ratio across heated tubes,

$$T = (T_o + T_a)\left[1 + \frac{\left(\frac{P_a}{P_o}\right)^{\frac{\delta-1}{\delta-1}}}{\eta}\right]$$, absolute air temperature at fan discharge, $^\circ R$,

$$t = \frac{T_1 + T_a}{T}$$, temperature ratio across heated tubes,

$$\overline{K} = (K_o + K_d)\,\nu^{-0.32}\left(\frac{T_1 + T_a}{T_{1r} + T_a}\right)^{0.23}$$, and

$$\nu = \frac{\nu + \left[\left(\frac{Cg_o}{RG^2}\right)\frac{P_a^2}{T}\,\frac{\left(1 - \frac{1}{r^2 t}\right)}{\left(1 + \frac{\ln(rt)}{\ln(r)}\right)\left(\ln(rt) + \frac{\overline{K}}{2}\right)}\right]^{1/2}}{2}$$, fan head.

The above equations are solved iteratively, using N iterations.

516 144

After N iterations and convergence the fan torque is determined by the following:

$$\beta = \begin{cases} \alpha^2 \sum_{i=1}^{5} C_i \left(\frac{\nu}{\alpha}\right)^{i-1}, & \nu \leq \alpha \\ \nu^2 \sum_{i=1}^{5} d_i \left(\frac{\alpha}{\nu}\right)^{i-1}, & \nu > \alpha \end{cases}.$$

Steady-State Equations (FAN3S)

The steady-state version of the subroutine calculates as follows:

$$\alpha = \begin{cases} \alpha_D & \text{if } K = 1 \\ 0 & \text{if } K = 0 \end{cases} \text{ relative fan speed.}$$

The vane angle θ is specified by a steady-state run. The fan flow, head, and torque; ν, δ, β, are determined iteratively in the same procedure as in the transient version of the subroutine.

Subroutine DAMP3T and DAMP3S

Defined Variables

These are the following:

L, lock open index, 0/1 = released/locked,

X_f, fine damper position,

X_c, coarse damper position, and

K_d, drag coefficient of dampers.

Required Variables

The following are computed by other subroutines:

α, fan speed,

K, fan breaker index, and

X, damper signal.

Input Parameters

a = 0.05, closed damper relative flow area,

α_1 = 0.20, fan speed to release damper lock,

α_2 = 0.25, fan speed required for damper lock,

X_ℓ = 0.85, coarse damper position required for damper lock,

τ = 20. , full range drive time, sec,

X_b = 0.50, break point between fine and coarse dampers, and

ε = 0.01, damper drive deadband.

Reference State Parameters and Variables

The reference state variables are:

L_r = 1 , reference lock open index (locked-open),

X_{fr} = 1.0 , reference fine damper position (open),

X_{fc} = 1.0 , reference coarse damper position (open), and

K_d = 0.0 , reference damper drag coefficient.

516 146

Transient Equations DAMP3T

The constant speed, sequential drive model used the following equations:

$L = 0$ if $K = 0$ or $\alpha \leq \alpha_1$, lock open circuit releases,

$L = 1$ if $K = 1$ and $\alpha \geq \alpha_2$ and $X \geq X_\ell$, lock open circuit engages,

$\frac{dX_f}{dt} = \frac{dX_c}{dt} = \frac{1}{\tau}$ if $L = 1$, dampers drive fully open if lock open circuit is engaged.

$X_{fd} = \frac{X}{X_b}$ and $X_{cd} = 0$ if $X \leq X_b$ and $L = 0$, the demanded damper positions when damper signal is less than the break point,

$X_{fd} = 1.0$ and $X_{cd} = \frac{X - X_b}{X_b}$ if $X > X_b$ and $L = 0$, the demanded damper positions when damper signal is greater than the break point,

$$\frac{dX_f}{dt} = \left\{ \begin{array}{l} \frac{1}{\tau}\ ,\ X_f < X_{fd} - \varepsilon \\ 0\ ,\ X_{fd} - \varepsilon \leq X_f \leq X_{fd} + \varepsilon \\ \frac{1}{\tau}\ ,\ X_f > X_{fd} + \varepsilon \\ \frac{1}{\tau}\ ,\ X > X_b \text{ and } X_f < 1, \end{array} \right\} \text{ if } X \leq X_b \text{ and } X_c = 0,$$

drives the fine dampers open or closed at a constant speed, and the following:

$$\frac{dX_c}{dt} = \left\{ \begin{array}{l} \frac{1}{\tau},\ X_c < X_{cd} - \varepsilon \\ 0,\ X_{cd} - \varepsilon \leq X_c \leq X_{cd} + \varepsilon \\ \frac{1}{\tau},\ X_c > X_{cd} + \varepsilon \\ \frac{1}{\tau},\ X \leq X_b \text{ and } X_c > 0, \end{array} \right\} \text{ if } X > X_b \text{ and } X_f = 1$$

drives the course dampers open or closed at a constant speed. The drag coefficient of the dampers is then calculated as

$$K_d = \left[1 - \frac{6}{8}(1 - a)\cos\left(\frac{X_c \pi}{2}\right) - \frac{2}{8}(1 - a)\cos\left(\frac{X_f \pi}{2}\right)\right]^{-2} - 1\ ,$$

where there are eight damper vanes, two of which are driven by the fine damper drive and the remaining six are driven by the coarse damper drive.

Steady-State Equations (DAMP3S)

In the steady state version, the lock open index L is determined from the same expressions as the transient version. The fine and coarse damper positions are determined as follows:

$$x_f = x_c = 1 \text{ if } L = 1,$$

$$x_f = \frac{x}{x_b},\ x_c = 0 \text{ if } L = 0 \text{ and } x \leq {}_b, \text{ and}$$

$$x_f = 1,\ x_c = \frac{x - x_b}{x_b} \text{ if } L = 0 \text{ and } x > x_b\ .$$

The drag coefficient K_d is determined from the same expression as the transient version.

REFERENCES

1. Division of Reactor Development & Technology, Fast Flux Test Facility, Summary Safety Report, USAEC, April 1971.

2. HEDL, Fast Flux Test Facility, System Design Description, No. 51, Heat Transport System, Rev. 31, October 1973.

3. R. B. Bird, W. E. Stewart, and E. N. Lightfoot, Transport Phenomena, J. Wiley & Sons, Inc., 1960.

4. A. P. Colburn, Trans. AIChE 29: 174 (1933).

5. Electric Machinery Manufacturing Company, Minneapolis, Minnesota, 200-syn-64 (1964).

6. HEDL, Fast Flux Test Facility, System Design Description, No. 90, Reactor Plant Control, Rev. 34, February 1975.

7. LMEC, FFTF HTS/DHX Prototype Module Testing in SCTI, Final Report, LMEC-76-4, February 1976.

8. S. L. Additon, T. B. McCall, C. F. Wolfe, Simulation of the Overall FFTF Plant Performance, HEDL TC-556, March 1976.

9. Fitzgerald & Kingsley, Electric Machinery, 2nd Edition, McGraw-Hill, 1961.

10. G. Kron, Equivalent Circuits of Electric Machinery, John Wiley & Sons, Inc., 1951.

11. C.P. Steinmetz, Theoretical Elements of Electrical Engineering, McGraw-Hill, 4th Edition, 1915.

12. Honeywell, Inc., Vutronik Cascade Central Stations, Operators Manual 37-01-05, April 1973.

13. K. R. Perkins, L. Chen, R. A. Bari,"Thermal Hydraulic Analysis of the Air Dump Heat Exchanger in the Fast Flux Test Facility," Trans. Am. Nucl. Soc. 28, 545 (June 1978).

14. K. K. Robinson, D. E. Briggs, Chem Eng. Proj. Symp., Ser. 62, 177 (1966).

15. D. E. Briggs, E. H. Young, Chem.Eng. Proj. Symp., Ser. 59, 1 (1965).

16. J. R. Dire, Test Report on DHX/HTS Fan, DTRF-458, January 1974.

17. American Warming and Ventilating, Inc., Test Report for Stack Outlet Dampers, QBN/14555

18. H. A. Backstrom, Calculated Torque vs Slip for Couplings: Revised Motor Time Acceleration Curve, Struthers-Wells Corp., DTRF-365, August 21, 1973.

516 149

DISTRIBUTION

Mr. J. Griffith, Chief (1)
LMFBR Branch
U.S. DOE
Washington, D.C. 20545

Assistant Director (1)
for CRBR Program Management
Division of Reactor Development
U.S. DOE
Washington, D.C. 20545

Assistant Director (1)
for FFTF Program Management
Division of Reactor Development
and Demonstration
U.S. DOE
Washington, D.C. 20545

Assistant Director (1)
for Engineering and Technology
Division of Reactor Development
and Demonstration
U.S. DOE
Washington, D.C. 20545

Assistant Director (1)
for Engineering
Division of Systems Safety
U.S. NRC
Washington, D.C. 20555

Mr. Robert Avery, Director (1)
Reactor Analysis & Safety
Division
Argonne National Laboratory
9700 South Cass Avenue
Argonne, Illinois 60439

Mr. L. W. Caffey, Director (1)
CRBRP Project Office, OR/RRD
P.O. Box U
Oak Ridge, Tennessee 37830

Dr. James Castle (1)
Department of Energy and Kinetics
University of California
at Los Angeles
Los Angeles, California 90024

Mr. R. T. Curtis (1)
Analytical Advanced Reactor
Safety Research Branch
Division of Reactor Safety Research
U.S. NRC
Washington, D.C. 20555

Mr. William D. Davey (1)
Fission Program Manager
University of California
Los Alamos Scientific Laboratory
P.O. Box 1663
Los Alamos, New Mexico 87544

Mr. W. P. Gammill (1)
Assistant Director for Standardization
and Advanced Reactors
Division of Project Management
U.S. NRC
Washington, D.C. 20555

Mr. H. Denton, Director (1)
Office of Nuclear Reactor Regulation
U.S. NRC
Washington, D.C. 20555

Director (1)
Neutron Physics Division
Oak Ridge National Laboratory
P.O. Box X
Oak Ridge, Tennessee 37830

Mr. Carl Erdman (1)
Department of Nuclear Engineering
University of Virginia, Thornton Hall
Charlottesville, Virginia 22901

Mr. R. Ferguson, Director (1)
FFTF Project Office RL/RRD
Richlands Operations Office
P.O. Box 555
Richland, Washington 99352

Mr. Stanley Goldsmith, Manager (1)
Fuels Design & Development Section
Battelle-Pacific Northwest Laboratories
Battelle Boulevard
Richland, Washington 99352

DISTRIBUTION (Cont.)

Mr. Paul Greebler, Manager (1)
General Electric Company
Nuclear and Safety Engineering
Fast Breeder Reactor Department
310 DeGuigne Drive
Sunnyvale, California 94086

Mr. R. J. Mattson, Director (1)
Division of Systems Safety
Office of Nuclear Reactor
Regulation
U.S. NRC
Washington, D.C. 20555

Professor David L. Hetrick (1)
Department of Nuclear Engineering
University of Arizona
Tucson, Arizona 85721

Mr. K. Hikido, Manager (1)
Systems Evaluation & Safety
Engineering
Fast Breeder Reactor Department
General Electric Company
310 DeGuigne Drive
Sunnyvale, California 94086

Mr. Harry Hummel (1)
Applied Physics Division
Argonne National Laboratory
Building 208
9700 South Cass Avenue
Argonne, Illinois 60439

Mr. M. G. Stevenson (1)
Los Alamos Scientific Laboratory
Los Alamos, New Mexico 87545

Mr. C. N. Kelber (1)
Assistant Director for Advanced
Reactor Safety Research
Division of Reactor Safety Research
U.S. NRC
Washington, D.C. 20555

Manager, Nuclear Safety (1)
Westinghouse Electric Corporation
Advanced Reactors Division
P.O. Box 158
Madison, Pennsylvania 15663

Mr. H. Morewitz (1)
Program Manager
LMFBR Physics and Safety
Atomics International
P.O. Box 309
Canoga Park, California 91304

Mr. J. F. Meyer (1)
Advanced Reactors Branch
Division of Project Management
U.S. NRC
Washington, D.C. 20555

Mr. D. F. Ross, (1)
Assistant Director for
Reactor Safety
Division of Systems Safety
U.S. NRC
Washington, D.C. 20555

Mr. M. Silberberg, Chief (1)
Experimental Fast Reactor
Safety Research Branch
Division of Reactor Safety Research
U.S. NRC
Washington, D.C. 20555

Mr. Daniel E. Simpson (1)
Manager, Safety Engineering
Hanford Engineering Development
Laboratory
P.O. Box 1970
Richland, Washington 99352

Mr. Themis P. Speis, Chief (1)
Advanced Reactors Branch
Division of Project Management
U.S. NRC
Washington, D.C. 20555

DISTRIBUTION (Cont.)

Technical Information Center, Chief (1)
U.S. NRC
P.O. Box 62
Oak Ridge, Tennessee 37830

Mr. R. Tedesco (1)
Assistant Director for Plant Systems
Division of Systems Safety
U.S. NRC
Washington, D.C. 20555

Mr. Theo G. Theofanous (1)
132 Pathway Lane
West Lafayette, Indiana 47906

U.S. NRC (5)
Secretary, Advisory Committee
on Reactor Safeguards
1717 H. Street, N.W.
Washington, D.C. 20555

Mr. Howard Holz (1)
Advanced Reactors Branch
Division of Project Management
U.S. NRC
Washington, D.C. 20555

Mr. Patrick O'Reilly (1)
Advanced Reactors Branch
Division of Project Management
U.S. NRC
Washington, D.C. 20555

Mr. Brian Sheron (1)
Analysis Branch
Division of Systems Safety
U.S. NRC
Washington, D.C. 20555

Mr. Phillip M. Wood (1)
Analytical Advanced Reactor
Safety Research
Division of Reactor Safety Research
U.S. NRC
Washington, D.C. 20555

Central Mail & Files (2)
U.S. Nuclear Regulatory Commission
Public Document Room
Washington, D.C. 20555

BNL DISTRIBUTION

A. K. Agrawal	(5)
K. B. Cady	(12)
H.J.C. Kouts	(1)
G. Brown, Lowell	(1)
J. E. Meyer, MIT	(1)
Code Development & Verification Group	(20)
RSP Division Heads	(4)
RSP Group Leaders	(5)
RSP Library	(2)